HSP90 is a therapeutic target in JAK2-dependent myeloproliferative neoplasms in mice and humans

Sachie Marubayashi,[1] Priya Koppikar,[1] Tony Taldone,[2] Omar Abdel-Wahab,[1,3] Nathan West,[4,5] Neha Bhagwat,[1,6] Eloisi Caldas-Lopes,[2] Kenneth N. Ross,[4] Mithat Gönen,[7] Alex Gozman,[2,8] James H. Ahn,[2] Anna Rodina,[2] Ouathek Ouerfelli,[9] Guangbin Yang,[9] Cyrus Hedvat,[10] James E. Bradner,[4,5] Gabriela Chiosis,[2] and Ross L. Levine[1,3]

[1]Human Oncology and Pathogenesis Program, [2]Molecular Pharmacology and Chemistry Program, and [3]Leukemia Service, Department of Medicine, Memorial Sloan-Kettering Cancer Center, New York, New York, USA. [4]Broad Institute of Harvard and Massachusetts Institute of Technology, Cambridge, Massachusetts, USA. [5]Department of Medical Oncology, Dana-Farber Cancer Institute, Boston, Massachusetts, USA. [6]Gerstner Sloan-Kettering Graduate School in Biomedical Sciences, New York, New York, USA. [7]Department of Epidemiology and Biostatistics, [8]Department of Pediatrics, [9]Organic Synthesis Core Facility, and [10]Department of Pathology, Memorial Sloan-Kettering Cancer Center, New York, New York, USA.

JAK2 kinase inhibitors were developed for the treatment of myeloproliferative neoplasms (MPNs), following the discovery of activating JAK2 mutations in the majority of patients with MPN. However, to date JAK2 inhibitor treatment has shown limited efficacy and apparent toxicities in clinical trials. We report here that an HSP90 inhibitor, PU-H71, demonstrated efficacy in cell line and mouse models of the MPN polycythemia vera (PV) and essential thrombocytosis (ET) by disrupting JAK2 protein stability. JAK2 physically associated with both HSP90 and PU-H71 and was degraded by PU-H71 treatment in vitro and in vivo, demonstrating that JAK2 is an HSP90 chaperone client. PU-H71 treatment caused potent, dose-dependent inhibition of cell growth and signaling in JAK2 mutant cell lines and in primary MPN patient samples. PU-H71 treatment of mice resulted in JAK2 degradation, inhibition of JAK-STAT signaling, normalization of peripheral blood counts, and improved survival in MPN models at doses that did not degrade JAK2 in normal tissues or cause substantial toxicity. Importantly, PU-H71 treatment also reduced the mutant allele burden in mice. These data establish what we believe to be a novel therapeutic rationale for HSP90 inhibition in the treatment of JAK2-dependent MPN.

Introduction

Myeloproliferative neoplasms (MPNs) comprise a group of clonal hematological malignancies that include chronic myeloid leukemia (CML), polycythemia vera (PV), essential thrombocytosis (ET), and primary myelofibrosis (PMF) (1, 2). Although the clonal, stem cell origin of these diseases was established more than 3 decades ago (3), the genetic basis of *BCR-ABL*–negative MPN remained elusive until several groups identified a somatic activating mutation in the JAK2 kinase (*JAK2V617F*) in the vast majority of patients with PV and in approximately 50% of ET and PMF patients (4–8). Subsequent studies have identified somatic mutations in exon 12 of JAK2 in *JAK2V617F*-negative PV (9) and in the thrombopoietin receptor (MPLW515L/K/A, MPLS505N) in a subset of *JAK2V617F*-negative ET and PMF, respectively (10–12). Expression of JAK2/MPL mutations in vitro allows hematopoietic cells to proliferate in the absence of cytokines and results in constitutive activation of signaling pathways downstream of JAK2, including the STAT3/5, MAP kinase, and PI3K signal transduction pathways (4, 13). Most importantly, expression of JAK2 or MPL mutations in vivo results in fully penetrant myeloproliferation, notable for polycythemia (JAK2V617F or JAK2 exon 12) (14–19) and/or thrombocytosis/myelofibrosis (JAK2V617F, MPLW515L) (10, 15). These data suggest constitutive JAK-STAT signaling is central to the pathogenesis of PV, ET, and PMF.

Although PV, ET, and PMF patients most commonly present with abnormalities on a complete blood count without associated symptoms, over time almost all patients develop symptomatic splenomegaly, thrombosis, bleeding, and/or infection. Most importantly, a significant proportion of patients develop progressive bone marrow failure and/or transformation to acute myeloid leukemia, which is associated with an extremely poor prognosis (20). Current therapies for PV and ET include antiplatelet therapy, phlebotomy, hydroxyurea, anagrelide, and IFN-α. These empiric treatments do not offer the possibility of clinical/molecular remission or cure, with the notable exception of the subset of patients who respond to chronic IFN-α therapy (21, 22). Treatment options for PMF are extremely limited for patients who are not candidates for allogeneic stem cell transplantation (23, 24). There is, therefore, a pressing need for novel therapies for MPN patients. The remarkable efficacy of tyrosine kinase inhibitors for CML and other MPNs (25) and the identification of mutations in the JAK2 signaling pathway in the majority of PV, ET, and PMF patients led to the development of JAK2 kinase inhibitors (26–28). Early data from phase I/II clinical trials in PMF and post-PV/ET myelofibrosis demonstrates that JAK2 inhibitor therapy can result in reductions in spleen size and in improvement in constitutional symptoms (29–31). However, to date, there have been minimal effects on the *JAK2V617F* allele burden and on peripheral blood cytopenias in the majority of patients in these trials. In addition, a significant proportion of patients have suffered hematopoietic toxicities, including anemia and thrombocytopenia, consistent with the known function of JAK2 signaling in normal erythropoiesis and thrombopoiesis (32). The limited efficacy of JAK2 inhibitors in the

Authorship note: Sachie Marubayashi and Priya Koppikar contributed equally to this work.

Conflict of interest: The authors have declared that no conflict of interest exists.

Citation for this article: *J Clin Invest.* 2010;120(10):3578–3593. doi:10.1172/JCI42442.

clinic provides impetus for the development of alternative therapeutic approaches for MPN patients that might prove effective when used alone or in combination with JAK2 kinase inhibitors.

We have thus devised an alternate strategy to antagonize aberrant tyrosine kinase signaling in MPN by targeting JAK2 oncoprotein stability with HSP90 inhibition. HSP90 is a ubiquitously expressed protein chaperone, which has been shown to stabilize a number of client proteins, including tyrosine kinases such as EGFR (33), BCR-ABL (34, 35), and FLT-3 (36). As a result, ATP-competitive HSP90 inhibitors, including the benzoquinone ansamycin 17-AAG and its derivates 17-DMAG and IPI-504, have been developed and investigated for the treatment of different malignancies (37). Early clinical results with the ansamycins have revealed dose-limiting nonhematopoietic toxicities (38), prompting the development of non-ansamycin HSP90 inhibitors such as PU-H71, SNX5422, and NVP-AUY922 (39). PU-H71 is a purine scaffold HSP90 inhibitor, which has demonstrated efficacy in preclinical models of triple-negative breast cancer (40) and diffuse large B cell lymphoma (41) through degradation of specific client proteins, including Akt and BCL-6, respectively. In addition, previous studies have demonstrated that, in comparison with ansamycin HSP90 inhibitors, PU-H71 demonstrates more favorable pharmacokinetic and pharmacodynamic properties, including avid, prolonged drug uptake by tumors that results in more potent and more sustained degradation of HSP90 client proteins (40), than those seen with 17-AAG and 17-DMAG dosed in vivo (42, 43). Moreover, the increased efficacy of PU-H71 in vivo is not associated with increased toxicity, as chronic PU-H71 therapy at doses effective in vivo is not associated with significant hematopoietic or nonhematopoietic toxicities (40). We therefore have undertaken assessment of the efficacy of HSP90 inhibition in JAK2-dependent malignancies, using PU-H71.

We report here significant antitumor activity of PU-H71 in MPN cell lines, in MPN murine models, and in primary MPN patient samples. PU-H71 treatment inhibited proliferation in cells expressing JAK2/MPL mutations at doses associated with degradation of JAK2 and with inhibition of downstream signaling pathways. Further, in vivo therapy with PU-H71 in mice expressing JAK2V617F or MPLW515L normalized peripheral blood counts, attenuated extramedullary hematopoiesis in both models, and improved survival compared with vehicle-treated mice in the MPLW515L model, all without associated hematopoietic or nonhematopoietic toxicity. Moreover, we demonstrate tumor-associated retention of PU-H71 and tumor-specific JAK2 degradation, which correlates with inhibition of JAK2/MPL mutant myeloproliferation, without significant effects on normal hematopoiesis. Of note, prolonged treatment with PU-H71 decreased the mutant allele burden in MPLW515L mice. Our data demonstrate that HSP90 inhibition represents an alternative approach to JAK2 inhibition of potential benefit for the treatment of patients with JAK2-dependent malignancies.

Results

HSP90 inhibition abrogates proliferation and signal transduction of JAK2/MPL mutant cell lines. Based on the above mechanistic rationale, we first studied a focused library of HSP90 inhibitors for their ability to inhibit the proliferation of Ba/F3 cells expressing JAK2/MPL mutations. Ba/F3 isogenic cell lines expressing JAK2V617F (IC_{50} = 29.0 nM) or MPLW515L (IC_{50} = 66.7 nM) were identified as highly sensitive to growth inhibition by PU-H71 (Figure 1A and Supplemental Figure 1; supplemental material available online with this article; doi:10.1172/JCI42442DS1). Similar results were obtained with 17-DMAG (Supplemental Figure 2A), demonstrating that growth inhibition of JAK2-dependent cell lines was observed with structurally divergent HSP90 inhibitors, supporting an on-target mechanism of action. Notably, the antiproliferative activity of HSP90 inhibition by PU-H71 in JAK2/MPL mutant Ba/F3 cells was more robust than that observed in control Ba/F3 cells expressing BCR-ABL, a widely studied, known client protein of HSP90 (IC_{50} = 110.1 nM) (Figure 1A and Supplemental Figure 1A). We next investigated the effects of PU-H71 in human leukemia cell lines in order to ascertain whether *JAK2* mutant human leukemia cell lines were sensitive to HSP90 inhibition. We found that *JAK2V617F* mutant cells, UKE-1 (IC_{50} = 116.7 nM) and SET-2 (IC_{50} = 94.1 nM), were more sensitive to PU-H71 than the *BCR-ABL*–positive KU812 cell line (IC_{50} = 312.8 nM) or the *JAK2/BCR-ABL*–negative THP-1 cell line (IC_{50} = 152.1 nM) (Figure 1A and Supplemental Figure 1A). PU-H71 treatment in vitro was associated with induction of apoptotic cell death at physiologically achievable concentrations (Supplemental Figure 3). We also investigated the effects of PU-H71 in MUTZ-5 cells, a human acute lymphoblastic leukemia (ALL) cell line recently described to have a *JAK2R683G* mutation (44–47), and found that this *JAK2* mutant lymphoid cell line was also sensitive to PU-H71 (IC_{50} = 123.8 nM) (Supplemental Figure 1A). These data demonstrate that JAK2V617F/MPLW515L mutant cells are uniformly sensitive to PU-H71 and suggest HSP90 inhibition may inhibit the proliferation of JAK2 mutant/dependent cells in additional malignancies.

We next investigated the effects of HSP90 inhibition on signal transduction pathways in JAK2/MPL mutant and wild-type hematopoietic cell lines. Treatment with PU-H71 markedly reduced phosphorylation of JAK2 in Ba/F3-EPOR-JAK2V617F and Ba/F3-MPLW515L cells (Figure 1B). We also observed dose-dependent inhibition of downstream signaling pathways, including phosphorylation of STAT3, STAT5, and MAP kinase, at physiologically achievable concentrations (Figure 1B). We observed potent inhibition of downstream signaling pathways in *JAK2V617F*-positive UKE-1 cells but not in *JAK2V617F*-negative THP-1 cells (Supplemental Figure 1B). Similar effects on signaling in Ba/F3 cells expressing JAK2/MPL mutations and in *JAK2V617F* mutant human leukemia cell lines were observed with 17-DMAG (Supplemental Figure 2B and data not shown).

JAK2 is a HSP90 client protein and associates with PU-H71/HSP90. Given that PU-H71 potently inhibited growth and signaling of the different JAK2-dependent cell lines, we next evaluated whether PU-H71–mediated HSP90 inhibition led to JAK2 degradation. Western blot analysis showed that PU-H71 or 17-DMAG treatment led to dose-dependent degradation of total JAK2 in both isogenic (Figure 1B and Supplemental Figure 2B) and leukemic cell lines (Supplemental Figure 1B and data not shown) at concentrations associated with inhibition of growth and signaling. Of note, degradation of both JAK2 and Raf1, a known HSP90 client protein (48–50), was observed at similar concentrations of PU-H71 (Figure 1B). We noted similar results in cells ectopically expressing MPLW515L alone or with overexpression of JAK2 (Figure 1B), demonstrating PU-H71 treatment leads to JAK2 degradation and inhibition of signaling in cells expressing endogenous or increased levels of JAK2. We next determined whether JAK2 is a bona fide HSP90 chaperone client protein. Immunoprecipitation experiments in Ba/F3 cells expressing JAK2/MPL mutants and in *JAK2V617F* mutant and wild-type leukemia cells demonstrated

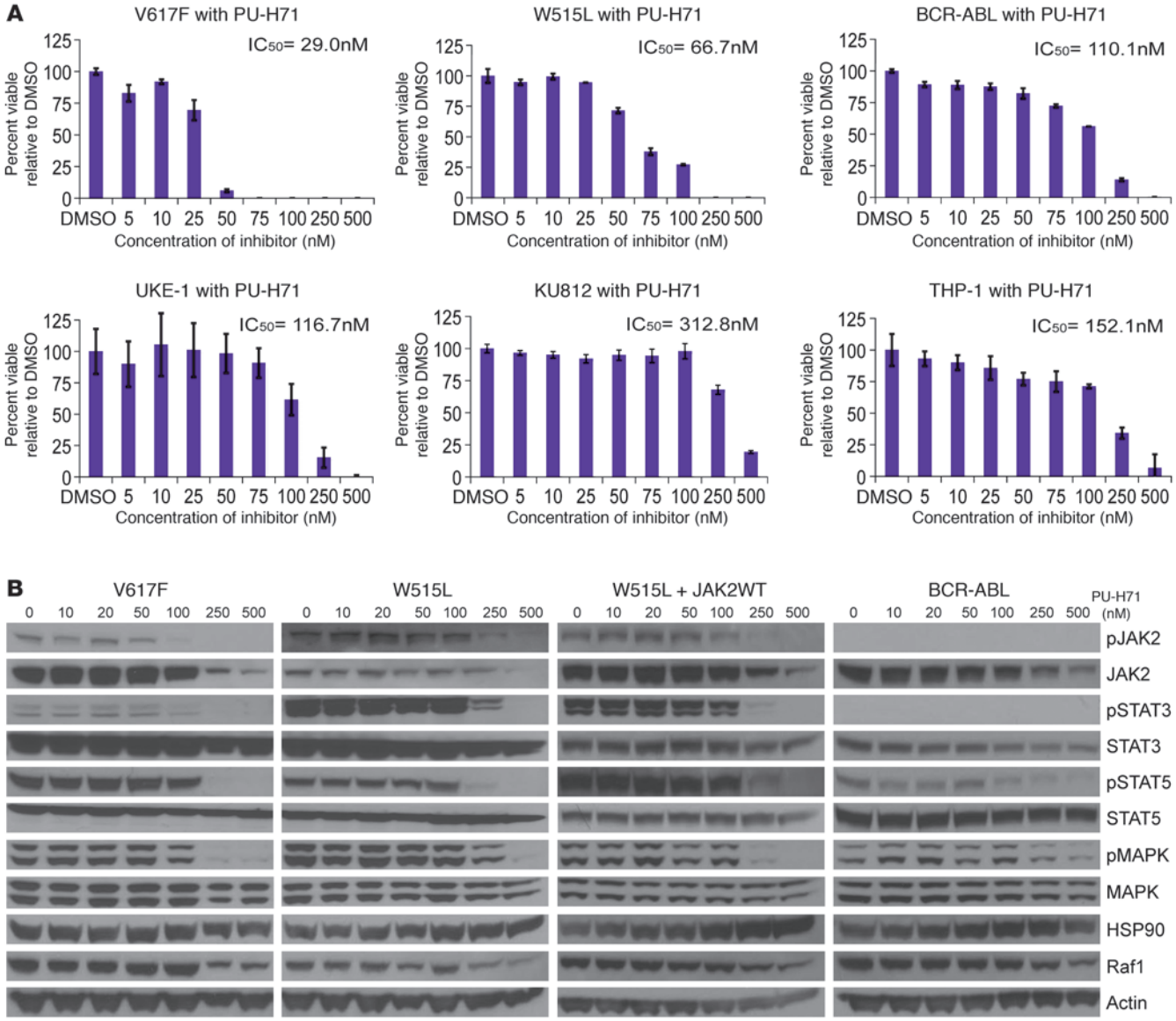

Figure 1

Effects on viability and signaling in MPN mutant cell lines treated with PU-H71. (**A**) Cells bearing mutations that result in constitutive activation of the JAK-STAT signaling pathway (JAK2V617F [V617F] and MPLW515L [W515L]) have a lower IC_{50} compared with that of Ba/F3 cells bearing BCR-Abl. Similarly, UKE-1 cells bearing JAK2V617F are more growth inhibited by PU-H71 than either KU812 (BCR-ABL) or THP-1 (JAK2 wild-type [JAK2WT]). (**B**) Western blots reveal a dose-dependent downmodulation of JAK2 and signaling intermediates in the JAK-STAT pathway after treatment with PU-H71 for 16 hours in Ba/F3 isogenic cell lines.

that JAK2 specifically associates with HSP90 (Figure 2A). Additionally, we demonstrated precipitation of JAK2 and HSP90 by PU-H71–coated agarose beads, confirming direct engagement of the JAK2-HSP90 complex by PU-H71 (Figure 2B).

Of note, PU-H71 treatment resulted in JAK2 degradation in JAK2 mutant, MPL mutant, and in JAK2 wild-type cells (Figure 1B and Supplemental Figure 1B). This suggested to us that unphosphorylated, wild-type JAK2 is also an HSP90 client protein; in support of this, we observed the association of JAK2, HSP90, and PU-H71 in *JAK2* wild-type THP-1 cells (Figure 2, A and B). To determine whether the interaction between HSP90 and JAK2 is affected by the phosphorylation status of JAK2, we pretreated *JAK2* wild-type THP-1 and *JAK2V617F* mutant UKE-1 cells (which have equivalent levels of JAK2 protein expression) with 5 μM of the JAK2 inhibitor TG101348 and then performed immunoprecipitation studies. We found that JAK2 and HSP90 associate in UKE-1 and THP-1 cells in the presence or absence of a JAK2 inhibitor, even at a concentration sufficient to completely inhibit JAK2 phosphorylation (Figure 2C). Next, we performed titration studies with PU-H71–coated agarose beads in order to determine whether limiting concentrations of PU-H71 associate with phosphorylated but not unphosphorylated JAK2. These studies showed that PU-H71 associates with JAK2 in a dose-dependent manner that is independent of JAK2 mutation or phosphorylation status (Figure 2D).

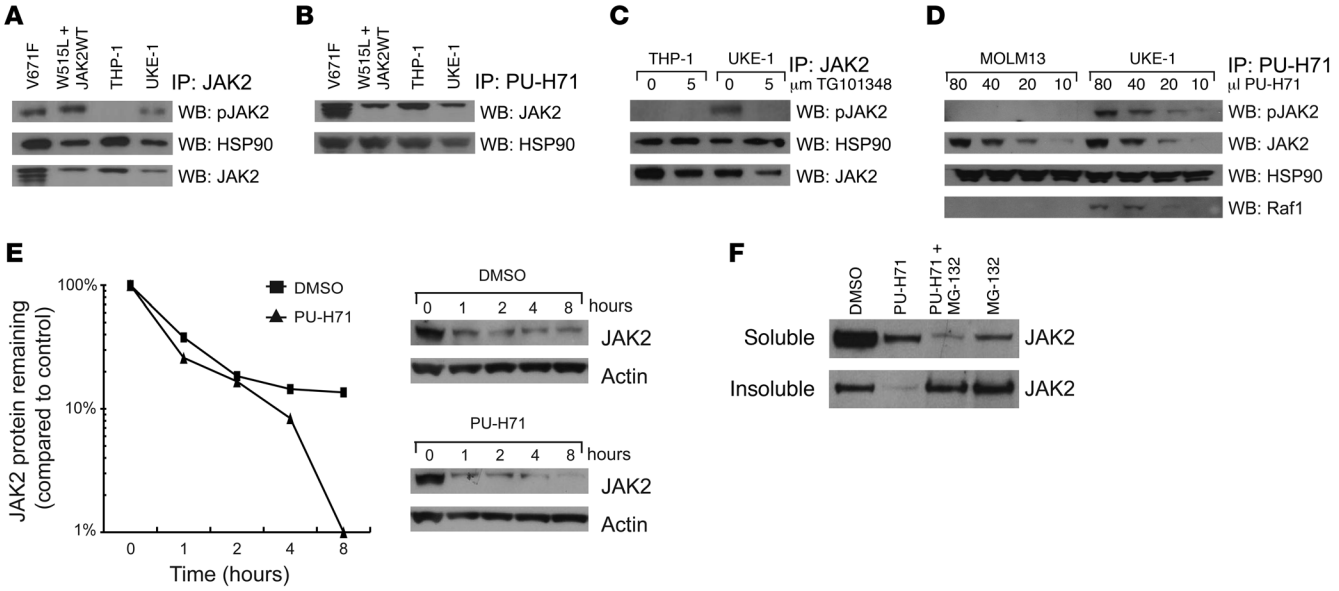

Figure 2

JAK2 associates with HSP90 and is degraded via the proteasomal pathway. (**A**) Ba/F3 isogenic and human leukemic cell lysates were immunoprecipitated with JAK2 and then probed for pJAK2, HSP90, and JAK2. (**B**) In a reciprocal experiment, cell lysates were incubated with PU-H71–conjugated beads and then blotted for JAK2 and HSP90. (**C**) THP-1 and UKE-1 cells were incubated with DMSO or 5 μM TG101348, a JAK2 inhibitor, for 4 hours, and then lysates were immunoprecipitated with JAK2, followed by Western blotting for pJAK2, HSP90, and JAK2. Association with HSP90 is not dependent upon phosphorylation. (**D**) Titration of PU-H71 beads does not change the kinetics of binding of PU-H71–conjugated beads with JAK2 or HSP90. Raf1, a known client protein of HSP90, is also shown. (**E**) Cycloheximide, a protein synthesis inhibitor, was used to determine the half-life of JAK2 protein. UKE-1 cells were pretreated with cycloheximide, along with either DMSO or 500 nM PU-H71, and harvested at different time points. Protein degradation began as early as 1 hour with PU-H71 treatment and was completely depleted after 8 hours of treatment. (**F**) UKE-1 cells were pretreated with 5 μM MG-132, before a 16-hour incubation with DMSO or 500 nM PU-H71. JAK2 expression was observed in the insoluble fraction with MG-132 treatment, showing that with PU-H71 treatment, JAK2 is degraded via the proteasomal pathway.

In order to better delineate the kinetics of JAK2 degradation, we assessed JAK2 protein levels at different times following incubation with PU-H71. We found that JAK2 protein levels begin to decrease within 4 hours of exposure to PU-H71 in *JAK2* mutant and wild-type cells (UKE-1 and KU812) (Supplemental Figure 4A). This was temporally associated with induction of HSP70 expression (Supplemental Figure 4A) and with inhibition of downstream signaling (data not shown). We did not observe changes in *JAK2* mRNA levels with 16 hours of PU-H71 exposure, at which time JAK2 protein levels were nearly undetectable (Supplemental Figure 4B). Consonant with the time course studies, we found that similar concentrations of PU-H71 were required to degrade JAK2 and to inhibit proliferation and signaling of JAK2/MPL mutant cells with 16 hours of exposure to PU-H71 (Supplemental Figure 4C).

The effects of PU-H71 on the stability of JAK2 were next assessed, using the protein biosynthesis inhibitor, cycloheximide. In the presence of cycloheximide, JAK2 is eliminated over 16 to 24 hours (Figure 2E and data not shown). PU-H71 treatment markedly increased the rate of JAK2 protein degradation, such that JAK2 protein was not detectable after 4–8 hours of drug exposure in treated cells (Figure 2E). These results demonstrate that PU-H71 specifically and rapidly degrades JAK2 in hematopoietic cell lines. We then investigated whether PU-H71–mediated degradation of JAK2 required the proteasomal degradation pathway, by investigating the effects of PU-H71 on JAK2 protein levels in *JAK2* mutant UKE-1 cells in the presence of the proteasome inhibitor, MG-132. Proteasome inhibition by MG-132 was found to prevent degradation of JAK2 prompted by PU-H71 (Figure 2F). Rather, MG-132 led to partitioning of JAK2 to the detergent insoluble fraction. In sum, these data support rapid and enhanced proteasomal degradation of JAK2 by PU-H71, consistent with prior studies of known HSP90 client proteins (49).

HSP90 inhibition and JAK2 kinase inhibition confer additive antiproliferative effects consistent with convergent effects on JAK-STAT signaling. Given that both HSP90 inhibitors and JAK2 kinase inhibitors inhibit growth and signaling in JAK2-dependent cells, we investigated the effects of combined JAK2 inhibitor and PU-H71 treatment in vitro. Using a high-throughput platform developed for the preclinical study of drug combinations, we assessed in parallel the individual and combined antiproliferative effects of PU-H71, a pan-JAK inhibitor (JAK Inhibitor I), and the JAK2-specific kinase inhibitor, TG101348, in pairwise dose-response studies in 8 experimental replicates in JAK2V617F mutant UKE-1 cells (Figure 3). We found that PU-H71, combined with either TG101348 (Figure 3A) or JAK Inhibitor I (Figure 3B), resulted in additive effects, as assessed by isobologram analysis using the median-effect principle of Chou and Talalay (51). These data emulate the observed effects of TG101348/JAK Inhibitor I combination studies (Figure 3C), which as expected revealed additive but not synergistic effects. These data suggest that HSP90 inhibitors and JAK2 kinase inhibitors elaborate common, on-pathway effects in JAK2-dependent MPN.

We further evaluated this finding by comparing the modulation of downstream transcriptional networks by HSP90 inhibition and JAK2 kinase inhibition, again using the investigative compound

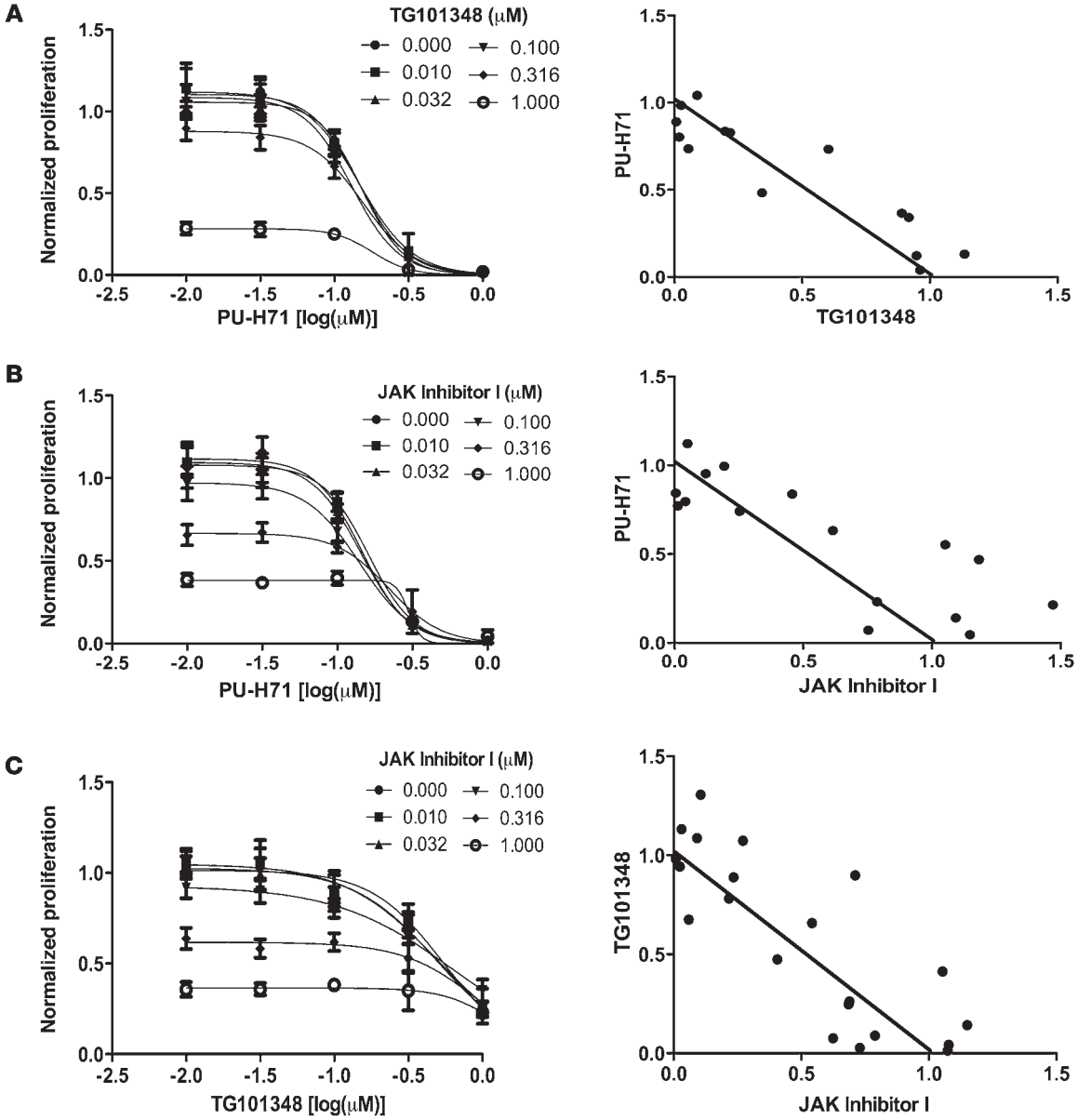

Figure 3

Combined inhibition of HSP90 and JAK2 impairs MPN cell proliferation. Pairwise dose-response data and isobologram synergy plots are presented for (**A**) PU-H71 and TG101348, (**B**) PU-H71 and Jak Inhibitor I, and (**C**) TG101348 and Jak Inhibitor I. Data are presented as mean measurements of the normalized proliferation of the UKE-1 cell line, treated for 72 hours, as determined by ATP content. Dose-response data are derived from a linear regression of 8 experimental replicates, plotted also with mean ± SD (GraphPad Prism). Normalized isobolograms are derived from matrix proliferation data analyzed using the median-effect principle of Chou and Talalay (Calcusyn). Error bars reflect SD calculated from 8 experimental replicates. The diagonal lines represent lines of additivity. Dots indicate paired values of drug concentrations assessed for synergism, using the median effect principle of Chou and Talalay. Additive and synergistic effects of the compounds are observed across a broad range of concentrations.

PU-H71 and JAK Inhibitor I, in UKE-1 cells. Hierarchical clustering revealed that PU-H71 and JAK2 inhibitor treatment in vitro led to global changes in gene expression; however, there was significant overlap between the PU-H71 and JAK2 inhibitor gene expression signatures (Figure 4A). Moreover, combined JAK2 kinase inhibitor and PU-H71 treatment led to similar changes in gene expression as those observed with PU-H71 treatment alone. We then used gene set enrichment analysis (GSEA) to assess the effects of PU-H71, JAK2 kinase inhibitor treatment, and combined PU-H71/JAK2 kinase inhibitor treatment on experimentally and computationally derived JAK-STAT gene expression signatures (52). Treatment with PU-H71 or with JAK Inhibitor I resulted in significant modulation of STAT-dependent target genes. Notably, the effects of PU-H71 on JAK-STAT target gene expression were more significant than those with JAK2 inhibitor treatment (Figure 4, B–D, and Table 1). Specifically, PU-H71 treatment significantly affected the expres-

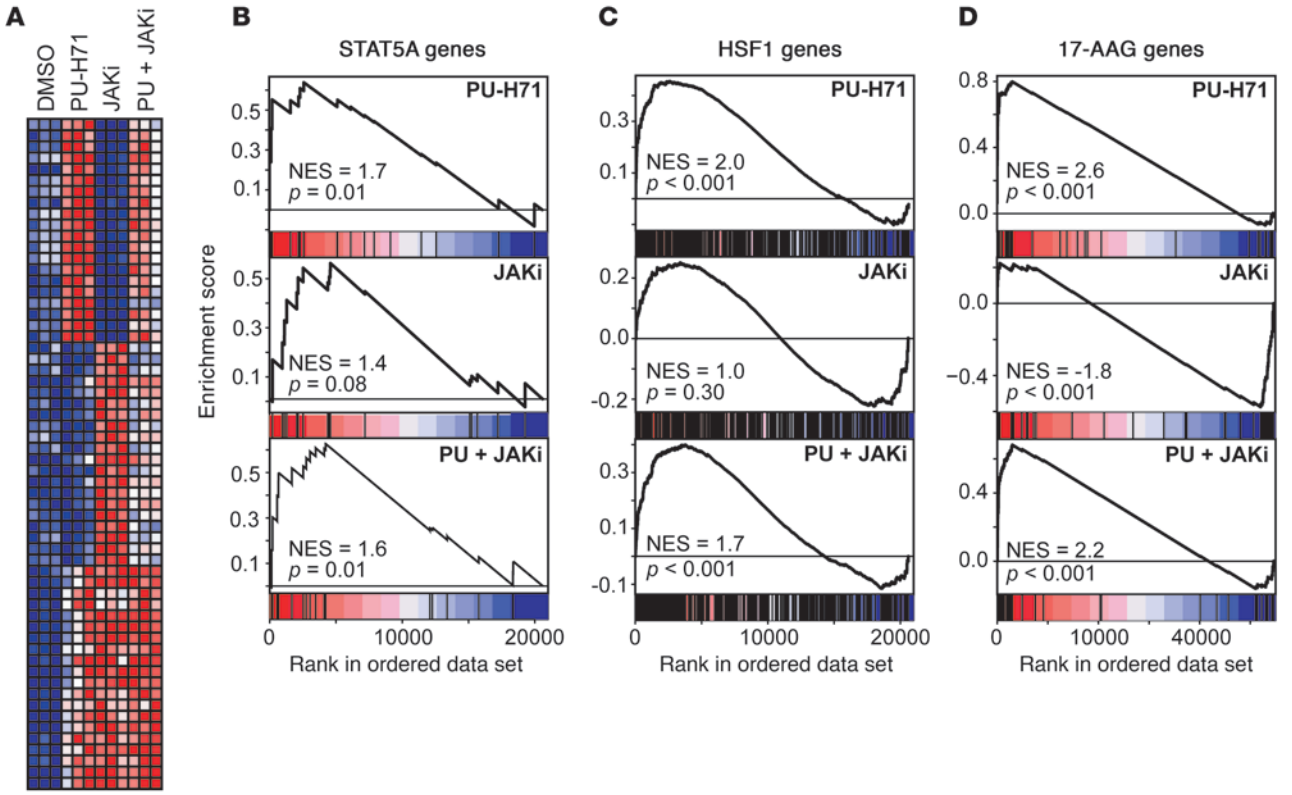

Figure 4

Inhibition of HSP90 by PU-H71 modulates the STAT5A transcriptional program. (**A**) Gene expression profiling was performed on the human leukemic cell line, UKE-1. UKE-1 cells were treated for 8 hours with DMSO, 250 nM PU-H71, 2 μM JAK Inhibitor I (JAKi), or a combination of both. The heat map presents the top 20 genes that discriminate between the treatment condition and control vehicle-treated samples. (**B**–**D**) Genes with increased expression are presented in red, whereas genes with decreased expression are shown in blue. GSEA was performed with each treatment condition to assess for modulation of (**B**) STAT5A target genes (**C**) HSF1 target genes and (**D**) genes modulated by exposure to the HSP90 inhibitor, 17-AAG. Graphical data represent enrichment scores across each genome-wide transcriptional profile and are annotated with normalized enrichment scores (NESs) and *P* values.

sion of both experimentally derived STAT5A targets (noted in Table 1 as Schuringa_STAT5A_DN) and computationally predicted STAT5A targets (noted in Table 1 as STAT5A_03, $P = 0.002$, STAT5A_04, $P < 0.001$) derived JAK-STAT gene expression signatures, whereas JAK2 inhibitor treatment had a significant effect on the gene expression signature based on computationally predicted STAT5A targets (STAT5A_03 and STAT5A_04, both $P < 0.001$) but not on expression of the genes in the experimentally derived gene expression signature (STAT5A_DN, $P = 0.08$) (52). In addition, combination PU-H71 and JAK2 kinase inhibitor treatment had similar effects on JAK-STAT target gene expression as those of PU-H71 alone. We then performed GSEA using a HSF1 (a transcription factor kept in an inactive state by HSP90) gene signature from the Molecular Signatures Database and using an experimentally derived 17-AAG gene expression signature derived from public data available through the Connectivity Map (http://www.broadinstitute.org/cmap/). As expected, treatment of cells with PU-H71, but not JAK2 kinase inhibitor, resulted in significant induction of HSF1-dependent target genes as well as expression of genes modulated by 17-AAG treatment in vitro (Figure 4, C and D). These data demonstrate that although treatment with PU-H71 has effects on gene expression not observed with JAK2 inhibitor treatment, PU-H71 and JAK2 inhibitors have similar effects on JAK-STAT target gene expression in JAK2-dependent hematopoietic cells, consistent with a shared

Table 1

Effects of JAK-STAT pathway inhibition on target gene expression

	PU-H71		JAKi		PU-H71 plus JAKi	
Gene set	**NES**	***P* value**	**NES**	***P* value**	**NES**	***P* value**
Schuringa_STAT5A_DN	–1.7	0.01	–1.4	0.08	–1.6	0.01
STAT5A_04	–1.7	< 0.001	–1.6	< 0.001	–1.6	< 0.001
STAT5A_03	–1.4	0.002	–1.5	< 0.001	–1.5	0.002
STAT5A_02	1.1	0.32	–1.0	0.41	–1.0	0.47
STAT5A_01	–1.0	0.60	–0.9	0.84	–0.9	0.68

Quantitative comparison of the functionally annotated target (Schuringa_STAT5A_DN) and computationally derived targets (STAT5A_01, STAT5A_02, STAT5A_03, and STAT5A_04). Gene set strings are provided for STAT5A signatures curated by the Molecular Signatures Database.

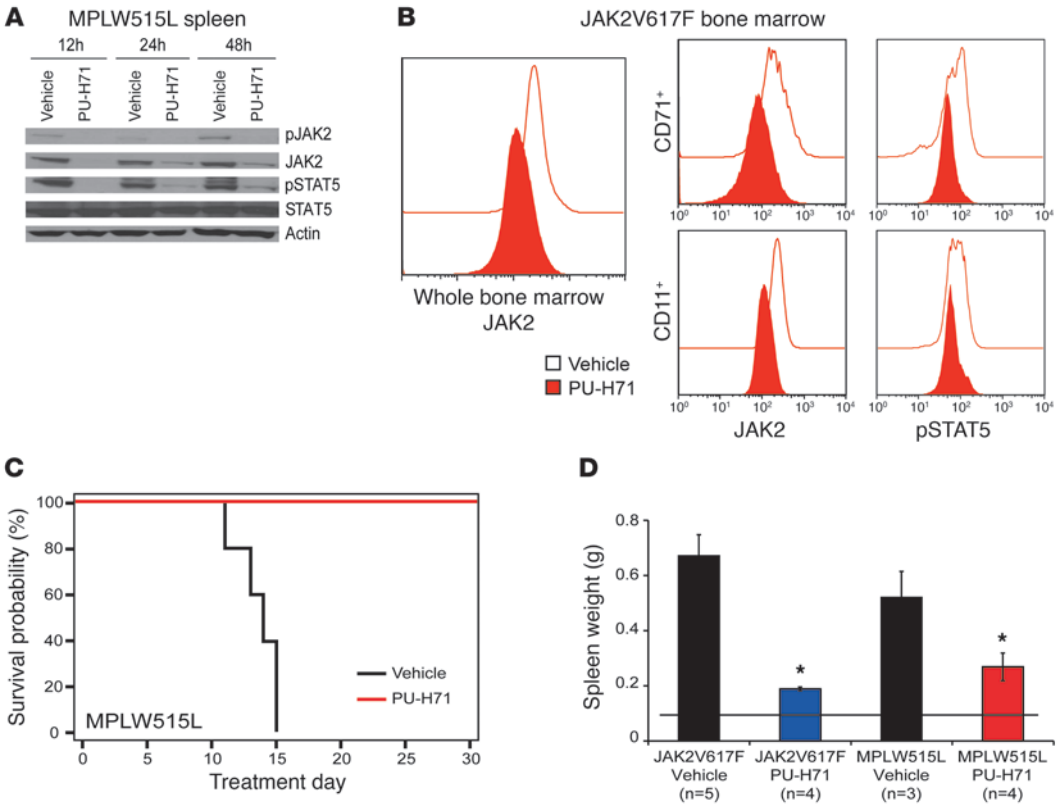

Figure 5

PU-H71 degrades JAK2 in vivo, reduces myeloproliferation, and improves survival. (**A** and **B**) Initial pharmacodynamic study of MPLW515L- and JAK2V617F-transduced spleen and bone marrow cells. (**A**) A single dose of 75 mg/kg PU-H71 for 12, 24, and 48 hours resulted in reduction in JAK2 and pSTAT5 levels, while actin is shown as loading control. (**B**) PU-H71–treated whole JAK2V617F bone marrow cells as well as the CD71 and CD11 fractions have decreased JAK2 and pSTAT5 expression in comparison with vehicle-treated JAK2V617F bone marrow when measured by flow cytometry. (**C**) Treatment with PU-H71 resulted in a significant increase in survival of MPLW515L mice compared with vehicle-treated MPLW515L mice as shown by the Kaplan-Meier survival curve ($P < 0.0004$, log-rank test). (**D**) Spleen weights of PU-H71–treated MPLW515L or JAK2V617F mice are significantly lower than those of vehicle-treated mice sacrificed at the same time (*$P < 0.01$). The horizontal line indicates the average weight of the normal BALB/c female mouse spleen at 8 weeks.

molecular target in this cellular context. Collectively, combination studies do not support enhanced inhibition of JAK-STAT signaling when adding a JAK2 kinase inhibitor to the HSP90 inhibitor, PU-H71, supporting plausible single-agent efficacy in MPN.

PU-H71 treatment degrades JAK2 in vivo and improves survival in MPN bone marrow transplant models. We next performed pharmacodynamic studies to investigate the effects of PU-H71 on JAK2 protein expression and on JAK-STAT signaling in vivo. We used the MPLW515L mouse retroviral bone marrow transplant model to rapidly induce leukocytosis and thrombocytosis in recipient mice (10) and sacrificed mice 12, 24, and 48 hours after a single intraperitoneal dose of 75 mg/kg PU-H71. We found that PU-H71 treatment resulted in degradation of JAK2 protein expression in vivo (Figure 5A), such that total JAK2 protein levels remained markedly suppressed in splenocytes from MPLW515L-transduced mice for at least 48 hours. This reduction in JAK2 protein levels correlated with inhibition of STAT5 phosphorylation in splenocytes from MPLW515L mutant mice for 48 hours after PU-H71 treatment, consistent with potent, on-target JAK2 inhibition (Figure 5A). We performed similar studies with mice engrafted with JAK2V617F-expressing bone marrow. Given that only a subset of bone marrow and splenocytes from mice transplanted with JAK2V617F-transduced cells are GFP positive (JAK2V617F is expressed using a MSCV-IRES-GFP virus), we used intracellular flow cytometry (53) to assess JAK2 protein levels and STAT5 phosphorylation in GFP-positive bone marrow, $CD71^+$ erythroid cells, and $CD11^+$ neutrophils in vehicle- and PU-H71–treated mice (Figure 5B). Compared with vehicle-treated mice, intracellular flow cytometry demonstrated that PU-H71 treatment resulted in marked reductions in JAK2 protein levels and STAT5 phosphorylation in the erythroid and granulocytic compartments. Of note, we subsequently adapted this assay for human cells (see below).

Based on these data, we implemented multidose efficacy studies. PU-H71 was administered at 75 mg/kg, 3 times weekly, based on prior studies, which demonstrated antitumor efficacy in cell line–derived xenograft models of breast cancer and lymphoma, without evidence of hematologic, renal, or hepatic toxicity (40, 41). We transplanted lethally irradiated mice with MPLW515L-expressing bone marrow, waited 12 days for all mice to develop significant leukocytosis, thrombocytosis, and splenomegaly, and then randomized mice to receive 28 days of vehicle or PU-H71. All MPLW515L mice treated with PU-H71 were alive for the entire 28-day treatment trial; whereas all vehicle-treated mice succumbed to disease by day 15 after treatment initiation (Figure 5C, $P < 0.0004$). Spleen weights were markedly

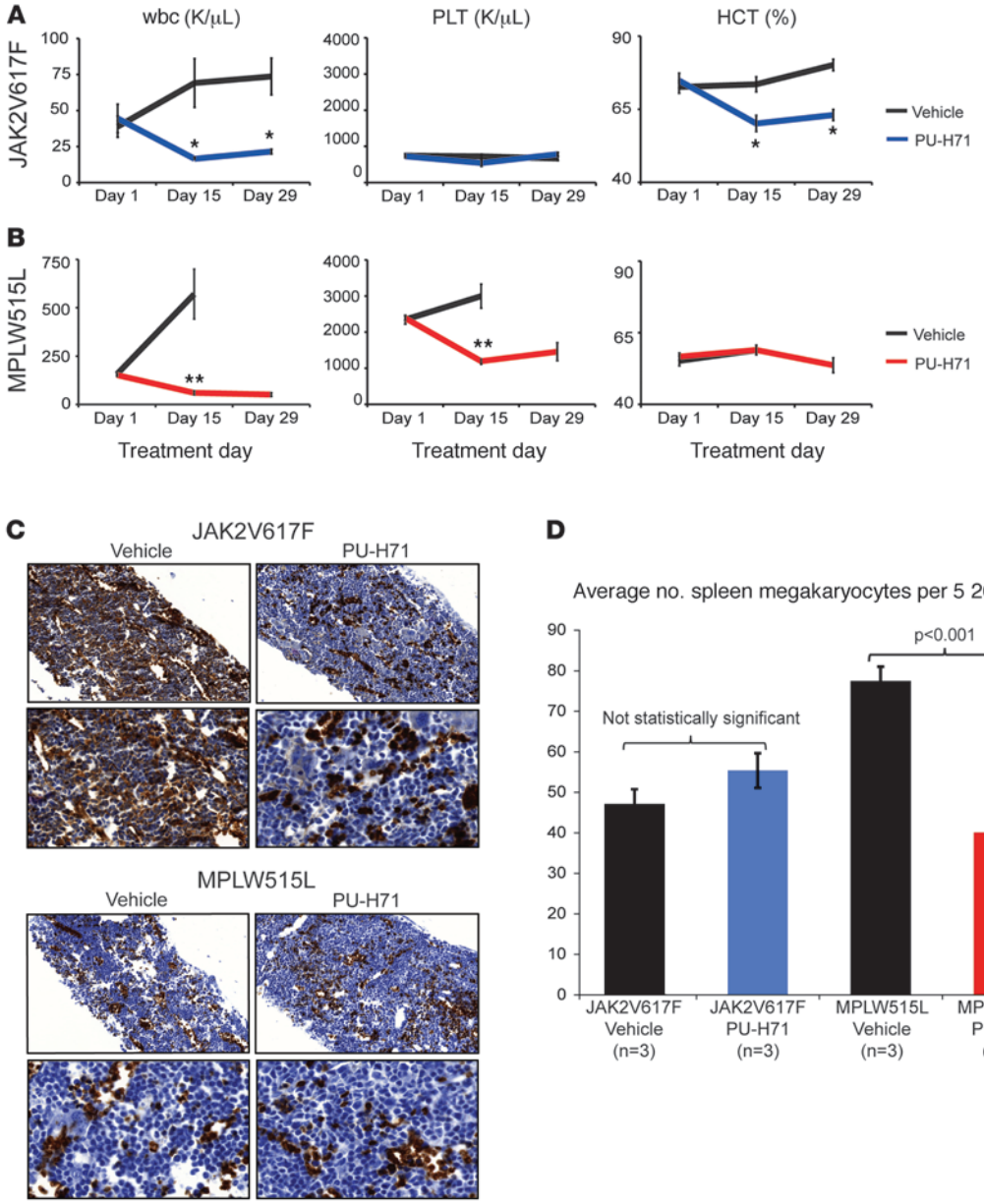

Figure 6

Lineage-specific reduction in myeloproliferation with PU-H71 treatment. (**A**) White blood cell count and hematocrit (HCT) values of PU-H71–treated JAK2V617F mice are lower in comparison with those of vehicle-treated mice, but there is no difference in the platelet (PLT) counts between both groups. *$P < 0.005$. (**B**) PU-H71–treated MPLW515L mice demonstrate reduced white blood cell and platelet counts, with unchanged hematocrit values over time. **$P < 0.01$. (**C**) Ter119 expression in PU-H71–treated bone marrow is reduced in comparison with vehicle-treated JAK2V617F bone marrow, while there are no significant differences between either vehicle- or drug-treated MPLW515L marrow. Original magnification, ×200 (top row); ×600 (bottom row). (**D**) PU-H71 significantly decreased the average number of megakaryocytes in spleens of MPLW515L mice ($P < 0.001$) but not JAK2V617F-treated mice.

reduced in PU-H71–treated mice transplanted with MPLW515L-expressing cells compared with vehicle-treated mice (Figure 5D, $P < 0.01$). We performed similar experiments with mice engrafted with JAK2V617F-expressing bone marrow cells. We waited for all mice injected with JAK2V617F-transduced bone marrow to develop polycythemia and leukocytosis and then randomized mice to receive 28 days of vehicle or PU-H71 treatment. As survival is not impaired in the first 2–3 months after injection with JAK2V617F-expressing cells, we assessed spleen weights in PU-H71– and vehicle-treated mice as a surrogate indicator of disease burden and found that PU-H71–treated JAK2V617F mice had marked reductions in spleen weight compared with those of vehicle-treated mice (Figure 5D, $P < 0.01$). These data demonstrate that PU-H71 improves survival in the MPLW515L bone marrow transplant model and reduces disease burden in the MPLW515L and JAK2V617F models.

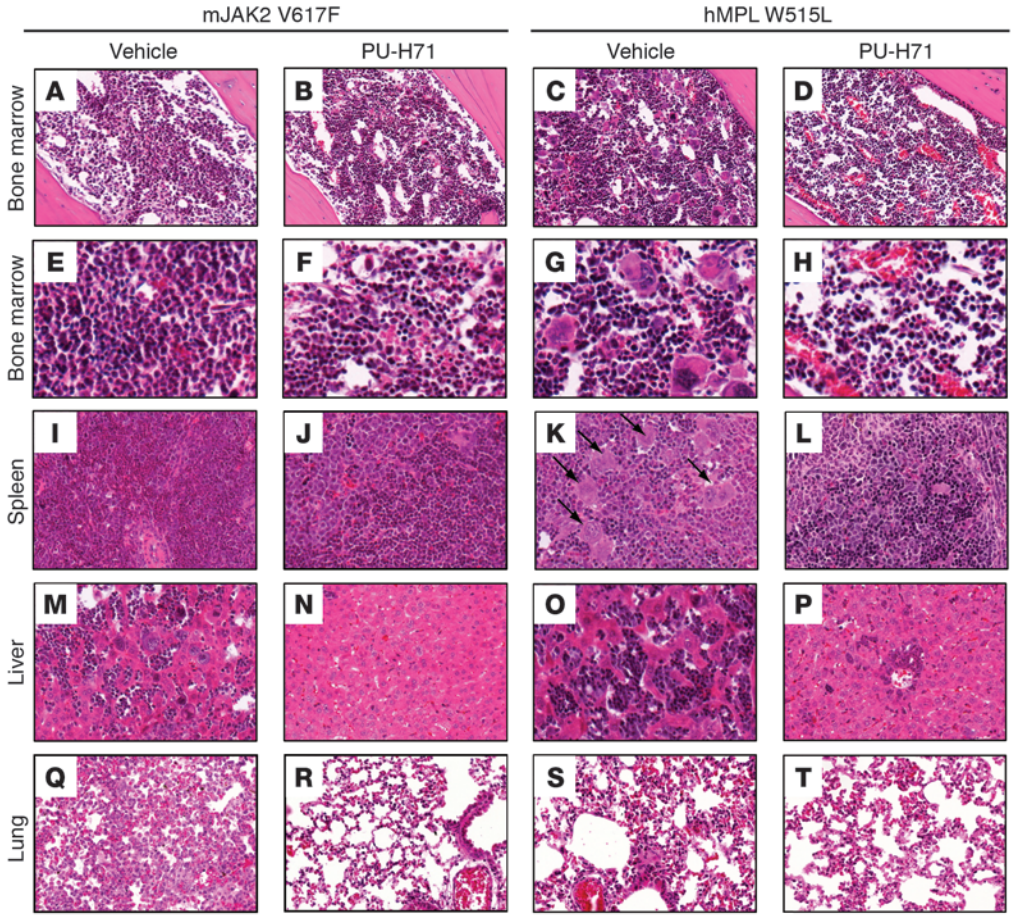

Figure 7

Histopathology of vehicle- and PU-H71–treated bone marrow, spleen, liver, and lung tissue. (**A**, **B**, **E**, and **F**) Tissue harvested at the same time demonstrated a slight decrease in cellularity between vehicle and PU-H71–treated JAK2V617F bone marrow. (**C**, **D**, **G**, and **H**) MPLW515L bone marrow showed a decrease in cellularity between vehicle- and PU-H71–treated tissue. (**I** and **J**) PU-H71–treated JAK2V617F spleen showed a reduction in myeloid infiltration as compared with vehicle-treated spleen. (**K** and **L**) PU-H71–treated MPLW515L spleen, on the other hand, showed fewer numbers of megakaryocytes (indicated by arrows). (**M**–**P**) There was extramedullary hematopoiesis in vehicle-treated JAK2V617F and MPLW515L liver that was reduced with PU-H71 treatment. (**Q**–**T**) Further, lung histopathology revealed an increase in neutrophils and extramedullary hematopoiesis in vehicle-treated JAK2V617F and MPLW515L mice that was decreased with PU-H71 treatment. Original magnification, ×200 (first, fourth, and fifth rows); ×400 (third row); ×600 (second row). mJAK2, mouse JAK2; hMPL, human MPL.

PU-H71 reduces lineage-specific myeloproliferation, without effects on normal erythropoiesis and megakaryopoiesis. We next assessed the effects of PU-H71 on myeloproliferation in vivo by measuring complete blood counts in MPLW515L- and JAK2V617F-expressing mice before, during, and after vehicle/PU-H71 treatment (Figure 6, A and B, and Supplemental Figure 5A). At the time treatment with vehicle or PU-H71 was initiated, all mice injected with JAK2V617F-transduced bone marrow had leukocytosis and polycythemia. Although white blood cell count and hematocrit levels continued to rise in vehicle-treated mice, PU-H71 treatment was associated with marked, sustained reduction in white blood counts (day 15, $P < 0.005$; day 29, $P < 0.005$) and in hematocrit levels (day 15, $P < 0.005$; day 29, $P < 0.005$) in all recipient mice (Figure 6A). Similarly, white blood cell and platelet counts continued to rise in vehicle-treated MPLW515L mice, whereas PU-H71 treatment was associated with significant reduction in white blood cell (day 15, $P < 0.01$) and platelet counts (day 15, $P < 0.01$) compared with vehicle treatment (Figure 6B). Importantly, PU-H71 treatment did not affect platelet counts in JAK2V617F mutant mice or hematocrit levels in MPLW515L mutant mice, suggesting the PU-H71 treatment schedule used in this trial specifically inhibited JAK2/MPL mutant–induced myeloproliferation, without appreciable affects on normal hematopoiesis.

To further investigate the lineage-specific effects of PU-H71 on JAK2/MPL mutant myeloproliferation, we performed additional analyses of in vivo erythropoiesis and megakaryopoiesis. Immunohistochemical analysis of PU-H71– and vehicle-treated bone marrow demonstrated a marked reduction in the proportion of Ter119-positive erythroid cells in PU-H71–treated JAK2V617F bone marrow compared with that of vehicle-treated bone marrow (Figure 6C). Differences in bone marrow Ter119 expression were not observed with PU-H71 treatment in MPLW515L bone marrow, consistent with the lack of an effect on erythropoiesis in MPLW515L mutant mice. Conversely, PU-H71 treatment was associated with a significant reduction in the number of megakaryocytes in the spleens of MPLW515L mice ($P < 0.001$), but not JAK2V617F mice again, consistent with inhibition of MPLW515L-induced pathologic megakaryopoiesis but not normal megakaryopoiesis (Figure 6D).

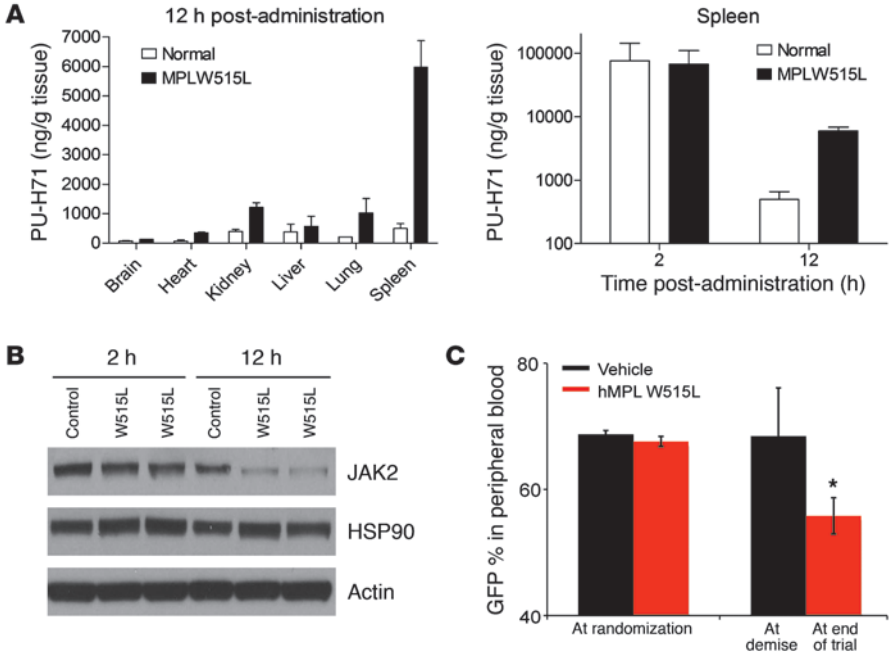

Figure 8
PU-H71 retention and allele burden in MPLW515L-transduced BALB/c mice. BALB/c mice were transplanted with both untransduced and MPLW515L-transduced bone marrow cells. Mice were sacrificed 2 or 12 hours after a single dose of 75 mg/kg PU-H71. Relevant tissues were harvested for LC-MS/MS analysis and Western blots. (**A**) LC-MS/MS results for relevant tissues over time. Spleen tissue in both control and MPLW515L mice at both 2 and 12 hours shows rapid uptake by 2 hours but only MPLW515L-specific accumulation of PU-H71 at 12 hours. (**B**) Western blotting of spleen tissue from control and MPLW515L mice at both 2 and 12 hours shows comparable levels of JAK2 at 2 hours, with a decrease in JAK2 levels in MPLW515L mice at 12 hours. Actin and HSP90 are shown as loading controls. (**C**) GFP percentage over time in both vehicle and 75 mg/kg PU-H71–treated MPLW515L mice. Initial levels of GFP are similar for both groups; however, over time there is a statistically significant decrease in the PU-H71–treated mice. *$P = 0.004$.

Pathologic and flow cytometric analyses of PU-H71–treated mice versus vehicle control mice. We then performed histopathologic analysis of vehicle- and PU-H71–treated mice. We noted a reduction in bone marrow cellularity (Figure 7, A, B, E, and F) and a reduction in myeloid infiltration of the spleens of PU-H71–treated JAK2V617F mice (Figure 7, I and J) compared with vehicle-treated mice. PU-H71 treatment was associated with reduction in bone marrow cellularity in MPLW515L mice (Figure 7, C, D, G, and H) and with reduced myeloid infiltration in the spleens (Figure 7, K and L) of MPLW515L mice. PU-H71 treatment was associated with decreased extramedullary hematopoiesis and neutrophilic infiltration in the liver and lungs of JAK2V617F (Figure 7, M, N, Q, and R) and MPLW515L mice (Figure 7, O, P, S, and T).

Consistent with histopathologic analyses, flow cytometric analysis of bone marrow and spleen revealed a marked decrease in the proportion of Gr1/Mac1-positive neutrophils in PU-H71–treated JAK2V617F and MPLW515L mice (Supplemental Figure 6, A and B). Further, we observed a decrease in the population of $CD71^+$ erythroid progenitor cells in the bone marrow of PU-H71–treated JAK2V617F mice and, to a lesser extent, PU-H71–treated MPLW515L mice (Supplemental Figure 6, C and D). Conversely, PU-H71 treatment was associated with a decrease in the proportion of bone marrow and spleen megakaryocyte progenitors ($CD61^+$ and $CD41^+CD61^+$ populations) in MPLW515L but not JAK2V617F mice (Supplemental Figure 6, E and F). PU-H71 treatment did not affect the proportion of B or T cell precursors in JAK2V617F and MPLW515L mice (Supplemental Figure 6, G and H, and data not shown).

PU-H71 is retained in MPN cells, leading to degradation of JAK2 in MPN cells but not normal cells. Although *Jak2* has been shown to be required for normal hematopoietic differentiation and is absolutely required for definitive erythropoiesis (32), PU-H71 specifically inhibited MPL/JAK2 mutant–mediated myeloproliferation, without apparent effects on normal hematopoiesis. We therefore chose to investigate the pharmacologic basis for the therapeutic window of PU-H71 in vivo. Given that we demonstrated JAK2 is a HSP90 client protein, regardless of mutational or activation status, and that both mutant and wild-type JAK2 are degraded by PU-H71, the basis for the selective effects of PU-H71 on MPN is likely not due to increased affinity of PU-H71 for mutant/active JAK2. Previous studies have shown that tumor-associated, hyperactive HSP90 has increased affinity in vivo for HSP90 inhibitors, leading to increased uptake of HSP90 inhibitors by metabolically active tumor cells (54). We therefore investigated whether tumor-selective accumulation of PU-H71 in vivo might result in tumor-specific JAK2 degradation, without affecting JAK2 protein levels in normal tissues. We performed bone marrow transplants with normal, untransduced bone marrow or with MPLW515L-transduced bone marrow and then waited for all mice to engraft and for the MPLW515L-transduced mice to develop disease. We then administered a single dose of PU-H71 (75 mg/kg) to mice injected with normal bone marrow and to mice with MPLW515L-induced myeloproliferation and used liquid chromatography tandem mass spectrometry (LC-MS/MS) to measure PU-H71 levels in target organs. Although PU-H71 was detectable in normal and diseased tissues 2 hours after drug administration, we saw marked, specific accumulation of PU-H71 in the spleens (Figure 8A) and bone marrow (Supplemental Figure 5B) of MPLW515L mice, but not normal mice, 12 hours after administration of the drug. Of note, we could detect more than 5 μg/g PU-H71 in the MPLW515L-transduced spleen 12 hours after a single dose of PU-H71, which corresponds to an in vivo concentration of more than 3 μM. We could detect modestly increased levels of PU-H71 in the liver, lung, and kidney of MPLW515L mice, consistent with myeloid infiltration of these target organs by MPL mutant cells, but we did not observed significant retention of PU-H71 in normal kidney, liver, or lung or retention of PU-H71 in brain or heart tissue isolated from normal or MPLW515L mice (Figure 8A). We also performed Western blot analysis of JAK2 protein levels in normal and MPLW515L splenocytes after a single dose of PU-H71. Consistent with the pharmacokinetic data, we observed potent degradation of JAK2

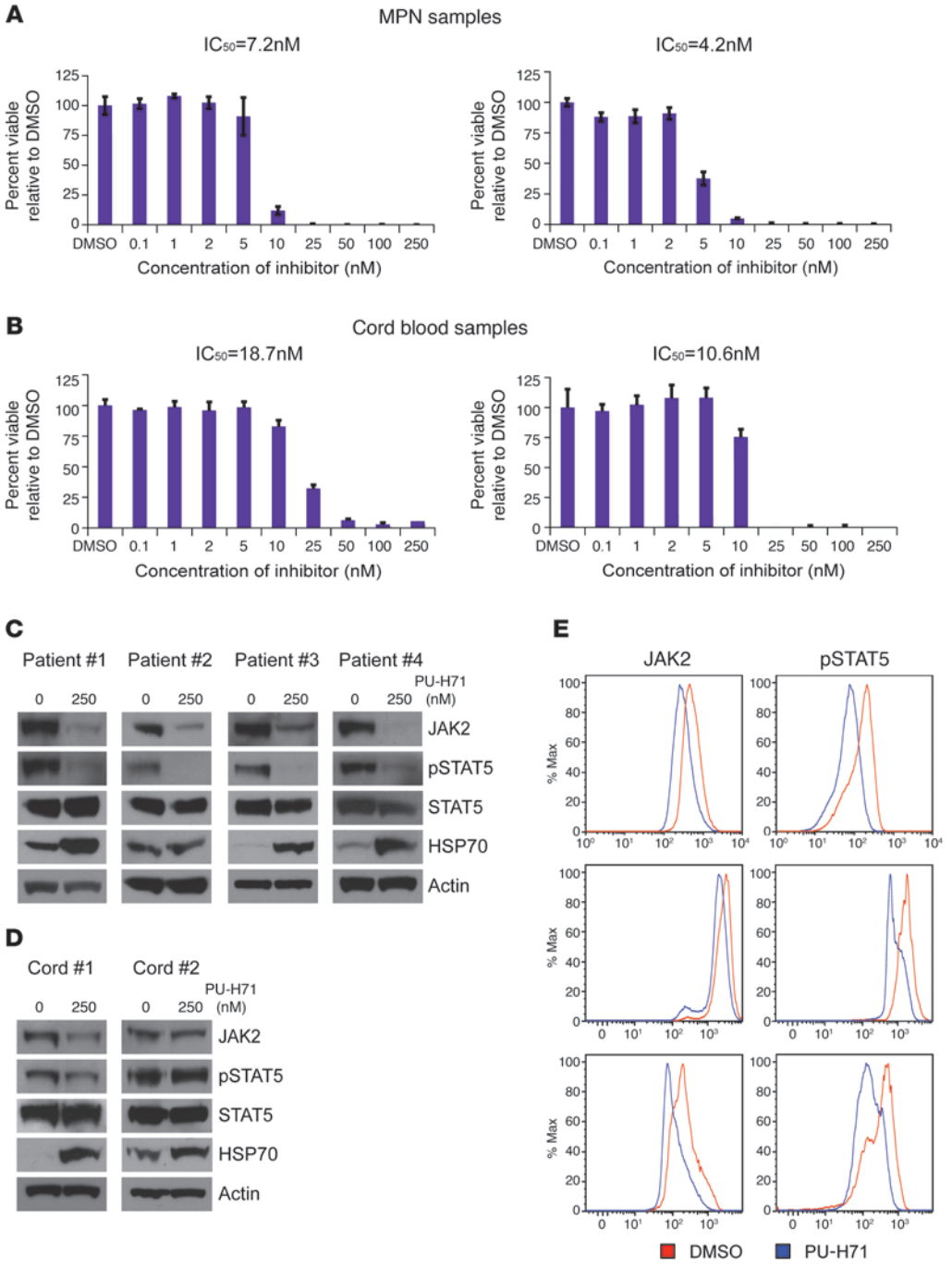

Figure 9

PU-H71 inhibits growth and signaling of JAK2V617F mutant MPN samples. (**A** and **B**) Viability assays of CD34 cells isolated from *JAK2V617F*-positive PV patients and normal cord blood cells show that the *JAK2V617F*-positive mutant cells are more sensitive to growth inhibition by PU-H71 than the CD34-positive cells isolated from normal cord blood. (**C** and **D**) Western blot analysis after treatment of the primary samples with either DMSO or 250 nM PU-H71 showed that JAK2 levels in PU-H71–treated patient samples were lower than those in normal cord blood samples. This decrease in JAK2 levels also correlated with increased inhibition of pSTAT5 and increased levels of HSP70 in these samples in comparison with cord blood samples. Total STAT5 and actin are shown as loading controls. (**E**) Flow cytometry revealed a decrease in both JAK2 and pSTAT5 levels in drug-treated patient samples.

in MPLW515L but not normal splenocytes 12 hours after administration of PU-H71 in vivo (Figure 8B). These data suggest that the prolonged retention of PU-H71 in MPN cells leads to potent degradation of JAK2 in a tumor-specific manner in vivo.

PU-H71 treatment decreases mutant allele burden in the MPLW515L murine model. In previous studies, we have observed that in vivo therapy with JAK2 inhibitors improves survival and reduces pathologic myeloproliferation in the MPLW515L MPN murine model

but does not result in reduction in the size of the malignant clone (55). We therefore wished to determine whether HSP90 inhibition with PU-H71 was able to reduce mutant allele burden in this model. As in previous studies with JAK2 inhibitors (55), we measured GFP expression over time as a surrogate marker of disease burden for MPLW515L mutant cells (MPLW515L is expressed using a MSCV-IRES-GFP virus). Vehicle and PU-H71 treatment groups had similar GFP percentages in peripheral blood before treatment. In contrast, PU-H71–treated mice, but not vehicle-treated mice, had a statistically significant reduction in GFP percentage over time (Figure 8C, $P = 0.004$). A similar reduction in GFP percentage was observed in splenocytes from PU-H71–treated mice, but not vehicle-treated MPLW515L mice, over time (data not shown).

PU-H71 inhibits growth and signaling of JAK2V617F mutant primary MPN samples. We next evaluated the effects of PU-H71 on the growth and signaling of primary MPN patient cells. We isolated CD34-positive cells from JAK2V617F primary patient samples and differentiated these cells into erythroid cells in serum-free medium with defined cytokines. CD34-positive cells isolated from cord blood samples of normal individuals were used as controls. We found that erythroid cells derived from MPN patients were 2- to 3-fold more sensitive to PU-H71 inhibition than normal cord blood cell samples (Figure 9, A and B). We then performed Western blot analysis after treatment with either DMSO or PU-H71 (250 nM) and found that PU-H71 treatment led to near-complete degradation of JAK2 in MPN patient samples (Figure 9C), with less significant JAK2 degradation observed in cord blood samples treated with PU-H71 (Figure 9D). Moreover, we noted that PU-H71 treatment resulted in inhibition of STAT5 phosphorylation in MPN patient samples but not cord blood samples, consistent with JAK2-dependent signaling by MPN cells (Figure 9, C and D). We noted induction of HSP70 in MPN patient samples and cord blood samples with PU-H71 treatment, a known pharmacodynamic measure of HSP90 inhibition. We were also able to confirm this data using phospho-flow analyses, which revealed a decrease in both JAK2 and pSTAT5 levels in drug-treated patient samples (Figure 9E).

Discussion

Genetic and functional studies have demonstrated the importance of JAK2/MPL mutations and resultant constitutive activation of JAK-STAT signaling to the pathogenesis of PV, ET, and PMF (56). This has led to the development of small molecule JAK2 inhibitors for the treatment of these MPNs, and several of these agents are in advanced clinical trials. Although existing JAK2 inhibitors demonstrate efficacy in a spectrum of in vitro and in vivo preclinical studies (27), to date clinical responses in PMF have been limited to reductions in spleen size and in systemic symptoms, without reductions in allele burden (29–31). Moreover, JAK2 inhibitor therapy has been associated with dose-limiting thrombocytopenia and anemia in a subset of patients. These data suggest that JAK2 kinase inhibitors may be limited in their efficacy, due to the requirement for JAK2 kinase activity in normal erythropoiesis and thrombopoiesis (32). In addition, we have observed that in vivo therapy with JAK2 inhibitors improves myeloproliferation but does not reduce mutant allele burden in the MPLW515L MPN murine transplant model (55). The inability of JAK2 kinase inhibitors to reduce mutant allele burden in vivo may be due to insufficient target inhibition at clinically achievable doses, the presence of additional mutations, the relatively short duration of therapy to date, or the incomplete dependence on JAK2 signaling by the MPN clone. Regardless, the clinical experience with JAK2 kinase inhibitors to date provides the impetus for the development of alternate therapeutic approaches for MPN patients.

In this report, we validate HSP90 as a therapeutic target in JAK2V617F and MPLW515L mutant MPN. We demonstrate that PU-H71, a purine scaffold HSP90 inhibitor, demonstrates efficacy in JAK2-dependent cell lines, in murine models of PV and ET, and in primary MPN patient samples. These effects were associated with dose-dependent, potent in vitro and in vivo inhibition of JAK2 activation and of downstream signaling pathways, including STAT3, STAT5, and MAPK signaling. Importantly, exposure to PU-H71 led to potent, dose-dependent degradation of JAK2 at doses similar to those required to degrade Raf1. Although previous studies have demonstrated that a spectrum of oncogenic tyrosine kinases, including FLT-3 (36) and BCR-ABL (34, 35), are HSP90 chaperone clients, in this study we provide biochemical evidence that JAK2 is a bona fide client of the HSP90 chaperone complex. We also show that HSP90 inhibitors degrade JAK2 and inhibit JAK-STAT signaling in vitro and in vivo. These data suggest that JAK2 protein stability is carefully regulated in MPN cells and may represent an Achilles' heel of JAK2-dependent malignancies that can be exploited for therapeutic benefit.

In vivo studies demonstrate that treatment with doses of PU-H71 that degrade JAK2 and inhibit JAK-STAT signaling markedly improves survival in the MPLW515L murine model. Moreover, we found that PU-H71 treatment causes inhibition of mutant-associated erythrocytosis and megakaryopoiesis in the JAK2V617F and MPLW515L murine models, respectively, without effects on normal erythrocytosis and megakaryopoiesis. Taken together, these data suggest HSP90 inhibitor therapy with PU-H71 has a specific effect on proliferation and signaling in the malignant clone. The selective effect of PU-H71 on JAK2/MPL mutant cells in vivo does not appear to result from increased dependence of mutant/activated JAK2 on the HSP90 chaperone complex. Rather, we show that PU-H71 is selectively retained in MPN cells and target tissues, and the tumor-selective accumulation of PU-H71 in vivo leads to selective JAK2 degradation. These data suggest that HSP90 inhibitors may have a broader therapeutic window than JAK2 inhibitors. Further, we also showed that unlike our previous studies with a JAK2 inhibitor (55), PU-H71 treatment leads to a decrease in mutant allele burden in the MPLW515L murine MPN model. These data provide a strong rationale for the clinical development of PU-H71 and other HSP90 inhibitors for the treatment of JAK2V617F/MPLW515L mutant MPN. In addition, flow cytometric assays for JAK2 protein expression and phospho-STAT5 and assessment of HSP70 induction can be used as pharmacodynamic assays for PU-H71 and other HSP90 inhibitors in early-phase clinical trials.

Given that PU-H71 and other HSP90 inhibitors degrade many different client proteins, it is likely that the effects of PU-H71 on myeloproliferation in vitro and in vivo may result from inhibition of multiple target proteins in MPN cells. However, several lines of data suggest that JAK2 is the key molecular target for HSP90 inhibitors in the context of JAK2/MPL-mediated myeloproliferation. First, PU-H71 led to dose-dependent JAK2 degradation and inhibition of oncogenic signaling pathways at similar doses in vitro and in vivo. Second, combination studies demonstrated that PU-H71 and 2 structurally divergent JAK2 kinase inhibitors were additive and not synergistic, consistent with a shared mechanism of action in this cellular context. Moreover, we observed similar effects on target gene expression with in vitro exposure to PU-H71

and a JAK2 inhibitor, although the effects of PU-H71 on STAT5 target gene expression were more pronounced than those with JAK2 inhibitor treatment. These data suggest that HSP90 inhibitors are likely to possess marked single-agent activity in JAK2/MPL mutant MPN. Certainly, in the event that these classes of agents have non-overlapping toxicity profiles, combination studies of HSP90 inhibitors and JAK2 kinase inhibitor should be pursued, so as to maximize target inhibition and to minimize toxicity.

Our study demonstrated specific efficacy of PU-H71 in MPN cell lines, murine models, and primary human samples, and so it is likely that PU-H71 and other HSP90 inhibitors will be of value for the treatment of other JAK2-dependent malignancies. Recent studies have identified activating mutations in JAK2 in a subset of patients with high-risk ALL (44–47), suggesting that HSP90 inhibition may be an important therapeutic strategy for patients with JAK2 mutant, refractory ALL. In addition, in vitro and in vivo studies have shown that a spectrum of solid tumors, including lung cancer, breast cancer, and prostate cancer, activate the JAK-STAT pathway through autocrine and paracrine mechanisms (57–59), and HSP90 inhibitors represent an alternative therapeutic approach, which can be used to inhibit JAK2 and other client proteins, which contribute to the pathogenesis of epithelial malignancies. Alternatively, PU-H71 can be used as a chemical probe to identify tumors dependent on HSP90 chaperone proteins, and these data can be integrated with genomic and proteomic studies in order to identify novel molecular targets in different human malignancies. Taken together, our data demonstrate the efficacy of HSP90 inhibition by PU-H71 in a genetically defined human malignancy and provide a compelling rationale for the immediate and targeted clinical development of HSP90 inhibitors in the treatment of MPNs.

Methods

Reagents. PU-H71 [8-(6-iodobenzo[d][1.3]dioxol-5-ylthio)-9-(3-(isopropylamino)propyl)-9H-purine-6-amine] was synthesized by the Chiosis Laboratory (60). One mM stock aliquots were prepared in DMSO, stored at –20°C, and diluted in appropriate media prior to use. For in vivo use, PU-H71 was formulated in 10 mM phosphate buffer at a pH of approximately 6.4. TG101348 (27) was synthesized in the Memorial Sloan-Kettering Cancer Center Organic Synthesis Core Facility; 1 mM stock aliquots were prepared in DMSO and diluted in appropriate media prior to use. The pan JAK inhibitor, JAK Inhibitor I, was purchased from Calbiochem (EMD Chemicals). Antibodies used for Western blotting and immunoprecipitation included pSTAT5 and phosphorylated and total JAK2, STAT3, MAPK, and AKT (all from Cell Signaling Technologies); STAT5 and Raf1 (both from Santa Cruz Biotechnology Inc.); HSP70 and HSP90 (both from StressMarq); and Actin (EMD Chemicals). The MSCV–mouse *JAK2V617F*–IRES-GFP (MSCV-m*JAK2V617F*-IRES-GFP) and MSCV–human *MPLW515L*–IRES-GFP (MSCV-*hMPLW515L*-IRES-GFP) plasmids have been described previously (10, 14). Luminescence assays were determined using Cell Titer-Glo (Promega). Information regarding the synthesis of TG101348 can be found in the Supplemental Methods.

Cell lines. 293T cells were grown in high glucose Dulbecco's modified Eagle's medium with 10% FBS. 293T cells were transiently cotransfected and retroviral supernatant was produced using Fugene 6 (Roche), according to manufacturer's procedure. Ba/F3 cells were transduced with MSCV-*hMPLW515L*-neo and MSCV-*hBCR-Abl*-neo, while Ba/F3 EPOR cells were transduced with MSCV-*mJAK2V167F*-neo and MSCV-*mJAK2K539L*-GFP viral supernatants. Ba/F3 cells were also doubly transduced with MSCV-*hMPLW515L*-neo and MSCV-*mJAK2WT*-puro and selected for growth in media containing both neomycin and puromycin. Transduced cells were cultured in RPMI-1640 with 10% FCS and subsequently flow sorted for GFP to determine viral transduction percentage.

The human leukemic cell lines KU812 (*BCR-Abl* positive) and SET-2 (*JAK2V617F* positive) were grown in RPMI-1640 with 20% FCS; whereas, THP-1 (*MLL-AF9*) and MOLM13 (*MLL-AF9, Flt3*) were grown in RPMI-1640 with 10% FCS. UKE-1 (*JAK2V617F*-positive) cells were grown in RPMI-1640 with 10% FCS, 10% horse serum, and 1 μM hydrocortisone. MPN samples were collected from patients who provided signed informed consent, under institutional review board–approved protocols at Memorial Sloan-Kettering Cancer Center. Umbilical cord blood from deidentified subjects was procured as a gift from the New York Blood Center. CD34 cells cultured from primary *JAK2V617F*-positive MPN patients and cord blood samples from normal donors were grown in StemSpan (StemCell Technologies) supplemented with IL-3, IL-6, and SCF for 5 days, followed by addition of Epo to enrich for erythroid progenitor cells as described previously (28).

In vitro inhibitor assays and Western blot analysis. Viable cells were plated at 10,000 cells per well in 96-well tissue culture–treated plates in 200 μl media with increasing concentrations of PU-H71 in triplicate. Primary cells were plated at a higher density of 50,000 cells per well and were cultured in cytokine-free media for the duration of the inhibitor assay. Forty-eight–hour inhibitor assays were assessed using the Cell viability luminescence assay. Results were normalized to growth of cells in media containing an equivalent volume of DMSO. The effective concentration at which 50% inhibition in proliferation occurred was determined using Graph Pad Prism 5.0 software.

For Western blot analysis, cells were harvested after treatment with various concentrations of PU-H71 for 16 hours. Cells were immediately centrifuged, washed in ice-cold PBS containing sodium orthovanadate, and collected in lysis buffer containing Protease Arrest (G-Biosciences), Phosphatase Inhibitor Cocktail II (EMD Chemicals), 1 mM Phenylmethylsulfonyl fluoride (MP Biomedicals), and 0.02 mM Phenylarsine oxide. Protein was normalized using the Bio-Rad Bradford protein estimation and separated using 4%–12% Bis-Tris electrophoresis gels (Invitrogen). Nitrocellulose membranes were blocked in TBS-T with 5% milk and incubated with appropriate dilutions of primary and secondary antibody.

Immunoprecipitation. Cells were harvested either at steady-state conditions or after 4 hours of incubation with a JAK2 inhibitor. Protein was normalized using the Bradford dye, and 500 μg of total protein was incubated either with PU-H71 beads for 4 hours or overnight with JAK2 antibody. For protein incubated overnight, protein G agarose beads (EMD Chemicals) were added for another 2 hours of incubation. After incubation, cells were washed thrice with cold PBS without Ca/Mg but with Laemmli buffer added, boiled for 12 minutes, and spun down, and supernatant was loaded onto gels and separated as previously described (see above). PU-H71 was immobilized onto solid-phase by covalent attachment to agarose beads (Affi-Gel 10, Bio-Rad) as previously described (40). 500 μg of protein lysate from isogenic and leukemic cells were then incubated with 30 μl of PU-H71–conjugated beads for 4 hours, followed by centrifugation and Western blot analysis for JAK2 and HSP90.

Protein half-life and proteasome-mediated degradation. UKE-1 cells were pretreated for 5 minutes with 100 mM Cycloheximide (Sigma-Aldrich) and subsequently incubated with either DMSO or 250 nM PU-H71 for various time points. Cells were harvested at 0, 1, 2, 4, 8, 16, and 24 hours and prepped for Western blots, as previously described (see above). For proteasome inhibitor studies, UKE-1 cells were pretreated with 5 μM MG-132 (EMD Chemicals) for 2 hours. Cells were then incubated for 16 hours with DMSO or 500 nM PU-H71. To isolate the detergent insoluble partition, cell

pellets were lysed in lysis buffer containing 2% SDS with repeated pipetting. Cell lysates were then quantitated, separated on SDS-PAGE gels, transferred to nitrocellulose membranes, blocked, and probed, as previously stated.

Densitometry. Western blots were scanned using Adobe Photoshop CS4 11.0.1, and quantitative densitometry was analyzed using the Un-Scan-It version 5.1. Each blot was normalized to actin and percent remaining was determined by amount of JAK2 in untreated cells.

Quantitative RT-PCR. Ba/F3 mutant cells expressing either V617F or W515L were incubated with either DMSO or 100 nM or 500 nM PU-H71 for 16 hours. Cells were harvested and RNA was extracted using the RNeasy Mini kit (Qiagen). RNA was reverse transcribed to cDNA using the Verso cDNA kit (ThermoFisher Scientific). Quantitative RT-PCR assays were performed using SYBR Green (Applied Biosystems). Transcript levels were normalized to endogenous levels of actin. The primers used for JAK2 were as follows: forward primer, 5′ GATGGCGGTGTTAGACATGA, and reverse primer, 5′ TGCTGAATGAATCTGCGAAA. Primers used for MPL were as follows: forward primer, 5′ CCTCACTCAGCCTCTGCTCT, and reverse primer, 5′ GAGGGAGATCCCATCAGGTT.

Transcriptional profiling and GSEA. UKE-1 cells were treated for 8 hours with PU-H71 (250 nM), JAK inhibitor I (2 μM), both agents in combination, or DMSO, in triplicate. Expression profiles were then generated by hybridizing processed RNA with Human Genome U133 Plus 2.0 arrays (Affymetrix). cDNA processing, chip preparation, hybridization, and chip scanning were performed at the Memorial Sloan-Kettering Cancer Center Core Facility. Raw CEL files were processed and normalized using Robust Multiarray Averaging (60). Expression data preprocessing, comparative marker selection analysis, and heat map visualizations were generated using GenePattern software (http://www.broadinstitute.org/cancer/software/genepattern/). Expression data was thresholded (10 minimum) and filtered (3-fold minimum change and 100 minimum absolute difference), leaving 709 probe sets out of the 54,675 probe sets on the U133 Plus 2.0 arrays. Comparative marker selection was performed on the data using signal-to-noise ratio, and the top 20 markers based upon signal-to-noise ratio were chosen after further filtering for *P* values of less than 0.05 and fold change between classes greater than 2.5 for the following 3 comparisons: DMSO-treated versus PU-H71– and JAK inhibitor–treated samples, DMSO-treated and PU-H71–treated versus JAK inhibitor–treated samples, and DMSO-treated and JAK inhibitor–treated versus PU-H71–treated samples. Signal-to-noise ratio is defined by the following equation:

$$S_i = \frac{\mu_{i1} - \mu_{i2}}{\sigma_{i1} + \sigma_{i2}} \quad \text{(Equation 1)}$$

where μ_{i1} represents the mean expression of samples from class 1 for feature i, σ_{i1} represents the SD of class 1 for feature i, and S_1 represents the signal-to-noise ratio. Supplemental Excel Files 1–3 show signal-to-noise ratio, *P* value, *q* value, and fold change for each of the selected features. *P* values were estimated from permutation tests that shuffled class labels. Multiple hypothesis testing was accounted for by examining the *q* value, where the *q* value is an estimate of the false discovery rate developed by Storey and Tibshirani (61). Resolution of the estimates of the *P* value and *q* value is limited by the number of samples available (9 total), but all selected features had *P* values of less than 0.05 and *q* values of less than 0.05. GSEA was performed using GSEA software (http://www.broadinstitute.org/gsea/). GSEA was performed using STAT and HSF1 gene sets from the Molecular Signatures Database (http://www.broadinstitute.org/gsea/msigdb/index.jsp) and a gene set for 17-AAG created using comparative marker selection, using the 17-AAG samples (15 samples) and corresponding DMSO controls (79 samples) from the Connectivity Map (http://www.broadinstitute.org/cmap/). (To create 17-AAG gene sets, Connectivity Map expression data was thresholded [10 minimum] and filtered [5-fold minimum change and 50 minimum absolute difference], after which comparative marker selection was performed using signal-to-noise ratio, where the top 50 markers were selected according to the signal-to-noise ratio after further filtering for *P* values of less than 0.005 and greater than 1.5-fold change between classes.) GSEA was performed with 2,500 gene set permutations and the weighted scoring metric. All probe sets, shown with the mean for each treatment condition and the corresponding *P* value, are presented in Supplemental Excel Files 1–3.

Synergy studies. UKE-1 cells were seeded in sterile, white, opaque 384-well microtiter plates (Corning), using an automated dispensing system (CyBi-Well, CyBio), at 1,000 cells per well. PU-H71, TG101348, and the Calbiochem JAK Inhibitor I were delivered by robotic pin transfer (60 nl) to achieve a matrix of pairwise dose-response incubations of each compound. Following incubation for 72 hours, ATP levels were determined for treated cells and controls (Cell Titer-Glo, Promega). Data were linked to experimental compound concentrations and normalized (Microsoft Excel). Dose-response curves were generated in Graph Pad Prism software. Combination indices were determined using the median-effect principle of Chou and Talalay (CalcuSyn Software). Isobologram plots were generated also in Graph Pad Prism software.

Murine model and analysis of mice. All animal studies were performed at Memorial Sloan-Kettering Cancer Center under an animal protocol approved by the Memorial Sloan-Kettering Cancer Center Instructional Animal Care and Utilization Committee. The JAK2V617F and MPLW515L murine BMT assay was performed as described previously (55). Briefly, bone marrow cells from 5-Flurouracil–treated (150 mg/kg) male donors were harvested and transduced with viral supernatant containing MSCV-*hMPLW515L*-IRES-GFP or MSCV-*mJAK2V617F*-IRES-GFP, and 7.5×10^5 cells were injected into the lateral tail veins of lethally irradiated (2×4.5 Gy) female BALB/c mice. For the JAK2V617F- and MPLW515L-transplanted mice, nonlethal bleeds were performed on day 46 and 12 after transplantation, respectively, to assess disease severity. Mice were then randomized to receive treatment with PU-H71 (75 mg/kg intraperitoneally, thrice weekly) or with vehicle (10 mM phosphate buffer, pH ~6.4), beginning 46 or 12 days after transplantation, for JAK2V617F and MPLW515L, respectively. With the exception of mice sacrificed at specific time points for flow cytometric analysis and histopathology, all mice were treated for 28 days or until any one of several criteria for sacrifice were met, including moribundity, more than 10% body weight loss, and palpable splenomegaly extending across the midline. Differential blood counts were assessed by submandibular bleeds before the trial, after 15 days of treatment/vehicle, and at study end points. Animal care was in strict compliance with institutional guidelines established by the Memorial Sloan-Kettering Cancer Center, the *Guide for the Care and Use of Laboratory Animals* (National Academy of Sciences [1996]), and the Association for Assessment and Accreditation of Laboratory Animal Care International. For histopathology, tissues were fixed in 4% paraformaldehyde and then embedded in paraffin for analysis. Tissue samples were stained using hematoxylin and eosin or ter119. Bone marrow and spleen cells were strained and viably frozen in 90% FCS and 10% DMSO.

Pharmacodynamic/pharmacokinetic studies. For pharmacodynamic and pharmacokinetic assays, recipient mice were injected with untransduced or MPLW515L-transduced bone marrow cells. After engraftment in all mice and disease initiation in MPLW515L mice, all mice were injected with 1 dose of PU-H71 (75 mg/kg intraperitoneally). Mice were euthanized by CO_2 asphyxiation and all relevant tissues were harvested 2 and 12 hours after PU-H71 administration. Tissue was flash frozen in liquid nitrogen, with a portion of spleen taken for Western analysis. Frozen tissue was dried and weighed prior to homogenization in acetonitrile/methanol (3:1) solution. Samples were vigorously vortexed for 30 seconds to allow complete release of PU-H71 from tissue and then spun down at 4°C. Concentrations of PU-H71 in tissue were determined by high-performance LC-MS/MS (40). PU-H71-d_6 was added as the internal standard (62). Compound analysis was performed

on the 6410 LC-MS/MS system (Agilent Technologies). A Zorbax Eclipse XDB-C18 column (2.1 × 50 mm, 3.5 μm) was used for the LC separation, and the analyte was eluted under an isocratic condition (65% H_2O plus 0.1% HCOOH: 35% CH_3CN) for 5 minutes at a flow rate of 0.35 ml/min.

Flow cytometry. Spleen and bone marrow cells were strained and washed in ice-cold PBS with 1% BSA. Cells were incubated with Fc block (BD Pharmingen) for 15 minutes, stained with monoclonal antibodies on ice for 20 minutes, washed again in ice-cold PBS with 1% BSA, and analyzed on a FACScan. All cells were gated using a viability marker (7-amino-actinomycin, EBiosciences) with at least 150,000 events gathered. Antibodies used were Ly-6 Gr-1 PE, CD41 PE, CD71 PE, ter119 APC Alexa Fluor 750, and CD4 (all from eBiosciences) and CD11b APC Cy7 and CD61 PE (both from BD Pharmingen). For phospho-flow analysis, fresh bone marrow cells or cultured primary cells were fixed in 2% paraformaldehyde (BD Pharmingen) and permeabilized with ice-cold 90% methanol. Briefly, cells were incubated with CD71 (FITC) (BD Pharmingen) in combination with anti–phospho-STAT5Y694 (Ax647) (BD Pharmingen) and total JAK2 (rabbit monoclonal, Cell Signaling Technologies). Cells were then washed and restained with goat anti-rabbit IgG (PECy5.5; Caltag Laboratories, Invitrogen). Following a final wash, cells were analyzed by flow cytometry on FACSCalibur flow cytometer. The gates for defining various subsets were set in the following manner, using (a) unstained controls, (b) "fluorescence-minus one" controls for experiments when more than 2 surface markers were used simultaneously, and (c) gating on discrete cell populations, when present, and then applying this exact gate to other groups stained with the same fluorophore. Also, all FACS data presented was gated on living cells, followed by gating for GFP-positive cells. Analysis was performed using FlowJo software, and results are shown as dot plots.

Statistics. Data is displayed as mean ± SEM. Statistical significance between 2 groups was assessed using the nonparametric exact 1-tailed (Mann-Whitney *U*) test to compare survival, blood counts, and megakaryocyte numbers between PU-H71– and vehicle-treated mice and using the signed ranks test and the exact reference distribution to compare spleen size and GFP percentage between PU-H71– and vehicle-treated mice. *P* values less than 0.05 were considered significant.

Acknowledgments

This work was supported by grants from the Leukemia Lymphoma Society to G. Chiosis and R.L. Levine and from the National Institutes of Health and the Howard Hughes Medical Institute to R.L. Levine. O. Abdel-Wahab is supported by the Clinical Scholars Program at Memorial Sloan-Kettering Cancer Center and by the American Society of Hematology. R.L. Levine is an Early Career Award recipient of the Howard Hughes Medical Institute and is the Geoffrey Beene Junior Chair at Memorial Sloan-Kettering Cancer Center. J.E. Bradner and N. West were supported by grants from the National Cancer Institute and the Burroughs-Wellcome Fund. A. Gozman and E. Caldas-Lopes were supported by a grant from the Clinical and Translation Science Center at Weill Cornell Medical College. We thank Neil Rosen and Charles Sawyers for their advice. We thank Agnes Viale and the Memorial Sloan-Kettering Cancer Center Genomics Core Facility for their help in performing the microarray experiments.

Received for publication January 25, 2010, and accepted in revised form July 21, 2010.

Address correspondence to: Ross L. Levine, Human Oncology and Pathogenesis Program, Memorial Sloan-Kettering Cancer Center, 1275 York Avenue, Box 20, New York, New York 10065, USA. Phone: 646.888.2796; Fax: 646.422.0890; E-mail: leviner@mskcc.org. Or to: Gabriela Chiosis, Molecular Pharmacology and Chemistry Program, Memorial Sloan-Kettering Cancer Center, 1275 York Avenue, New York, New York 10065, USA. Phone: 646.888.2238; Fax: 646.422.0416; E-mail: chiosisg@mskcc.org. Or to: James E. Bradner, Department of Medical Oncology, Dana-Farber Cancer Institute, 44 Binney Street, Boston, Massachusetts 02115, USA. Phone: 617.632.6629; Fax: 617.582.7370; E-mail: james_Bradner@dfci.harvard.edu.

1. Dameshek W. Some speculations on the myeloproliferative syndromes. *Blood*. 1951;6(4):372–375.
2. Campbell PJ, Green AR. The myeloproliferative disorders. *N Engl J Med*. 2006;355(23):2452–2466.
3. Adamson JW, Fialkow PJ, Murphy S, Prchal JF, Steinmann L. Polycythemia vera: stem-cell and probable clonal origin of the disease. *N Engl J Med*. 1976;295(17):913–916.
4. James C, et al. A unique clonal JAK2 mutation leading to constitutive signalling causes polycythaemia vera. *Nature*. 2005;434(7037):1144–1148.
5. Baxter EJ, et al. Acquired mutation of the tyrosine kinase JAK2 in human myeloproliferative disorders. *Lancet*. 2005;365(9464):1054–1061.
6. Kralovics R, et al. A gain-of-function mutation of JAK2 in myeloproliferative disorders. *N Engl J Med*. 2005;352(17):1779–1790.
7. Levine RL, et al. Activating mutation in the tyrosine kinase JAK2 in polycythemia vera, essential thrombocythemia, and myeloid metaplasia with myelofibrosis. *Cancer Cell*. 2005;7(4):387–397.
8. Zhao R, et al. Identification of an acquired JAK2 mutation in polycythemia vera. *J Biol Chem*. 2005;280(24):22788–22792.
9. Scott LM, et al. JAK2 exon 12 mutations in polycythemia vera and idiopathic erythrocytosis. *N Engl J Med*. 2007;356(5):459–468.
10. Pikman Y, et al. MPLW515L is a novel somatic activating mutation in myelofibrosis with myeloid metaplasia. *PLoS Med*. 2006;3(7):e270.
11. Pardanani AD, et al. MPL515 mutations in myeloproliferative and other myeloid disorders: a study of 1182 patients. *Blood*. 2006;108(10):3472–3476.
12. Beer PA, et al. MPL mutations in myeloproliferative disorders: analysis of the PT-1 cohort. *Blood*. 2008;112(1):141–149.
13. Lu X, et al. Expression of a homodimeric type I cytokine receptor is required for JAK2V617F-mediated transformation. *Proc Natl Acad Sci U S A*. 2005;102(52):18962–18967.
14. Wernig G, Mercher T, Okabe R, Levine RL, Lee BH, Gilliland DG. Expression of Jak2V617F causes a polycythemia vera-like disease with associated myelofibrosis in a murine bone marrow transplant model. *Blood*. 2006;107(11):4274–4281.
15. Lacout C, Pisani DF, Tulliez M, Gachelin FM, Vainchenker W, Villeval JL. JAK2V617F expression in murine hematopoietic cells leads to MPD mimicking human PV with secondary myelofibrosis. *Blood*. 2006;108(5):1652–1660.
16. Bumm TG, et al. Characterization of murine JAK2V617F-positive myeloproliferative disease. *Cancer Res*. 2006;66(23):11156–11165.
17. Zaleskas VM, et al. Molecular pathogenesis and therapy of polycythemia induced in mice by JAK2 V617F. *PLoS ONE*. 2006;1:e18.
18. Tiedt R, et al. Ratio of mutant JAK2-V617F to wild-type Jak2 determines the MPD phenotypes in transgenic mice. *Blood*. 2008;111(8):3931–3940.
19. Xing S, et al. Transgenic expression of JAK2V617F causes myeloproliferative disorders in mice. *Blood*. 2008;111(10):5109–5117.
20. Tam CS, et al. The natural history and treatment outcome of blast phase BCR-ABL- myeloproliferative neoplasms. *Blood*. 2008;112(5):1628–1637.
21. Kiladjian JJ, et al. Pegylated interferon-alfa-2a induces complete hematologic and molecular responses with low toxicity in polycythemia vera. *Blood*. 2008;112(8):3065–3072.
22. Quintas-Cardama A, et al. Pegylated interferon alfa-2a yields high rates of hematologic and molecular response in patients with advanced essential thrombocythemia and polycythemia vera. *J Clin Oncol*. 2009;27(32):5418–5424.
23. Rondelli D, et al. Allogeneic hematopoietic stem-cell transplantation with reduced-intensity conditioning in intermediate- or high-risk patients with myelofibrosis with myeloid metaplasia. *Blood*. 2005;105(10):4115–4119.
24. Tefferi A. New insights into the pathogenesis and drug treatment of myelofibrosis. *Curr Opin Hematol*. 2006;13(2):87–92.
25. Druker BJ, et al. Efficacy and safety of a specific inhibitor of the BCR-ABL tyrosine kinase in chronic myeloid leukemia. *N Engl J Med*. 2001; 344(14):1031–1037.
26. Pardanani A, et al. TG101209, a small molecule JAK2-selective kinase inhibitor potently inhibits myeloproliferative disorder-associated JAK2V617F and MPLW515L/K mutations. *Leukemia*. 2007;21(8):1658–1668.
27. Wernig G, et al. Efficacy of TG101348, a selective JAK2 inhibitor, in treatment of a murine model of JAK2V617F-induced polycythemia vera. *Cancer Cell*. 2008;13(4):311–320.
28. Hexner EO, et al. Lestaurtinib (CEP701) is a JAK2 inhibitor that suppresses JAK2/STAT5 signaling and the proliferation of primary erythroid cells from patients with myeloproliferative disorders.

Blood. 2008;111(12):5663–5671.
29. Verstovek S, et al. Long-term follow up and optimized dosing regimen of ICNB018424 in patients with myelofibrosis: durable clinical, functional and symptomatic responses with improved hematological safety. *Blood (ASH Annual Meeting Abstracts)*. 2009;114:756.
30. Pardanani A, et al. A phase I evaluation of TG101348, a selective JAK2 inhibitor, in myelofibrosis: clinical response is accompanied by significant reduction in JAK2V617F allele burden. *Blood (ASH Annual Meeting Abstracts)*. 2009;114:755.
31. Hexner E, et al. A multicenter, open label phase I/II study of CEP701 (Lestaurtinib) in adults with myelofibrosis; a Report On Phase I: A Study of the Myeloproliferative Disorders Research Consortium (MPD-RC). *Blood (ASH Annual Meeting Abstracts)*. 2009;114:754.
32. Parganas E, et al. Jak2 is essential for signaling through a variety of cytokine receptors. *Cell*. 1998; 93(3):385–395.
33. Sawai A, et al. Inhibition of Hsp90 down-regulates mutant epidermal growth factor receptor (EGFR) expression and sensitizes EGFR mutant tumors to paclitaxel. *Cancer Res*. 2008;68(2):589–596.
34. An WG, Schulte TW, Neckers LM. The heat shock protein 90 antagonist geldanamycin alters chaperone association with p210bcr-abl and v-src proteins before their degradation by the proteasome. *Cell Growth Differ*. 2000;11(7):355–360.
35. Gorre ME, Ellwood-Yen K, Chiosis G, Rosen N, Sawyers CL. BCR-ABL point mutants isolated from patients with imatinib mesylate-resistant chronic myeloid leukemia remain sensitive to inhibitors of the BCR-ABL chaperone heat shock protein 90. *Blood*. 2002;100(8):3041–3044.
36. George P, et al. Cotreatment with 17-allylaminodemethoxygeldanamycin and FLT-3 kinase inhibitor PKC412 is highly effective against human acute myelogenous leukemia cells with mutant FLT-3. *Cancer Res*. 2004;64(10):3645–3652.
37. Neckers L. Hsp90 inhibitors as novel cancer chemotherapeutic agents. *Trends Mol Med*. 2002; 8(4 suppl):S55–S61.
38. Solit DB, et al. Phase I trial of 17-allylamino-17-demethoxygeldanamycin in patients with advanced cancer. *Clin Cancer Res*. 2007;13(6):1775–1782.
39. Chiosis G, et al. A small molecule designed to bind to the adenine nucleotide pocket of Hsp90 causes Her2 degradation and the growth arrest and differentiation of breast cancer cells. *Chem Biol*. 2001;8(3):289–299.
40. Caldas-Lopes E, et al. Hsp90 inhibitor PU-H71, a multimodal inhibitor of malignancy, induces complete responses in triple-negative breast cancer models. *Proc Natl Acad Sci U S A*. 2009;106(20):8368–8373.
41. Cerchietti LC, et al. A purine scaffold Hsp90 inhibitor destabilizes BCL-6 and has specific antitumor activity in BCL-6-dependent B cell lymphomas. *Nat Med*. 2009;15(12):1369–1376.
42. Eiseman JL, et al. Pharmacokinetics and pharmacodynamics of 17-demethoxy 17-[[(2-dimethylamino)ethyl]amino]geldanamycin (17DMAG, NSC 707545) in C.B-17 SCID mice bearing MDA-MB-231 human breast cancer xenografts. *Cancer Chemother Pharmacol*. 2005;55(1):21–32.
43. Solit DB, et al. 17-Allylamino-17-demethoxygeldanamycin induces the degradation of androgen receptor and HER-2/neu and inhibits the growth of prostate cancer xenografts. *Clin Cancer Res*. 2002;8(5):986–993.
44. Russell LJ, et al. Deregulated expression of cytokine receptor gene, CRLF2, is involved in lymphoid transformation in B-cell precursor acute lymphoblastic leukemia. *Blood*. 2009;114(13):2688–2698.
45. Mullighan CG, et al. Rearrangement of CRLF2 in B-progenitor- and Down syndrome-associated acute lymphoblastic leukemia. *Nat Genet*. 2009;41(11):1243–1246.
46. Hertzberg L, et al. Down syndrome acute lymphoblastic leukemia, a highly heterogeneous disease in which aberrant expression of CRLF2 is associated with mutated JAK2: a report from the International BFM Study Group. *Blood*. 2010; 115(5):1006–1017.
47. Yoda A, et al. Functional screening identifies CRLF2 in precursor B-cell acute lymphoblastic leukemia. *Proc Natl Acad Sci U S A*. 2010;107(1):252–257.
48. da Rocha Dias S, Friedlos F, Light Y, Springer C, Workman P, Marais R. Activated B-RAF is an Hsp90 client protein that is targeted by the anticancer drug 17-allylamino-17-demethoxygeldanamycin. *Cancer Res*. 2005;65(23):10686–10691.
49. Grbovic OM, et al. V600E B-Raf requires the Hsp90 chaperone for stability and is degraded in response to Hsp90 inhibitors. *Proc Natl Acad Sci U S A*. 2006;103(1):57–62.
50. Solit DB, et al. Phase II trial of 17-allylamino-17-demethoxygeldanamycin in patients with metastatic melanoma. *Clin Cancer Res*. 2008;14(24):8302–8307.
51. Chou TC, Talalay P. Quantitative analysis of dose-effect relationships: the combined effects of multiple drugs or enzyme inhibitors. *Adv Enzyme Regul*. 1984;22:27–55.
52. Schuringa JJ, Chung KY, Morrone G, Moore MA. Constitutive activation of STAT5A promotes human hematopoietic stem cell self-renewal and erythroid differentiation. *J Exp Med*. 2004;200(5):623–635.
53. Irish JM, et al. Single cell profiling of potentiated phospho-protein networks in cancer cells. *Cell*. 2004;118(2):217–228.
54. Kamal A, et al. A high-affinity conformation of Hsp90 confers tumour selectivity on Hsp90 inhibitors. *Nature*. 2003;425(6956):407–410.
55. Koppikar P, et al. Efficacy of the JAK2 inhibitor INCB16562 in a murine model of MPLW515L-induced thrombocytosis and myelofibrosis. *Blood*. 2010;115(14):2919–2927.
56. Levine RL, Pardanani A, Tefferi A, Gilliland DG. Role of JAK2 in the pathogenesis and therapy of myeloproliferative disorders. *Nat Rev Cancer*. 2007;7(9):673–683.
57. Pedranzini L, et al. Pyridone 6, a pan-Janus-activated kinase inhibitor, induces growth inhibition of multiple myeloma cells. *Cancer Res*. 2006;66(19):9714–9721.
58. Gao SP, et al. Mutations in the EGFR kinase domain mediate STAT3 activation via IL-6 production in human lung adenocarcinomas. *J Clin Invest*. 2007;117(12):3846–3856.
59. Hedvat M, et al. The JAK2 inhibitor AZD1480 potently blocks Stat3 signaling and oncogenesis in solid tumors. *Cancer Cell*. 2009;16(6):487–497.
60. Irizarry R, et al. Exploration, normalization, and summaries of high density oligonucleotide array probe level data. *Biostatistics*. 2003;4(2):249–264.
61. Storey JD, Tibshirani R. Statistical significance for genomewide studies. *Proc Natl Acad Sci U S A*. 2003;100(16):9440–9445.
62. Taldone T, Zatorska D, Kang Y, Chiosis G. A facile and efficient synthesis of d6-labelled PU-H71, a purine scaffold Hsp90 inhibitor. *J Labelled Comp Radiopharm*. 2010;53(1):47–49.